Chemical Engineering Journal 414 (2021) 128872

Contents lists available at ScienceDirect

Chemical Engineering Journal

journal homepage: www.elsevier.com/locate/cej

Review

Sulfite-based advanced oxidation and reduction processes for water treatment

Shaohua Wu [a,b,c], Leyuan Shen [b], Yan Lin [a,b], Kai Yin [b], Chunping Yang [a,b,c,d,*]

[a] Guangdong Provincial Key Laboratory of Petrochemcial Pollution Processes and Control, School of Environmental Science and Engineering, Guangdong University of Petrochemical Technology, Maoming, Guangdong 525000, China
[b] College of Environmental Science and Engineering, Hunan University and Key Laboratory of Environmental Biology and Pollution Control (Hunan University), Ministry of Education, Changsha, Hunan 410082, China
[c] Maoming Engineering Research Center for Organic Pollution Control, Maoming, Guangdong 525000, China
[d] Hunan Provincial Environmental Protection Engineering Center for Organic Pollution Control of Urban Water and Wastewater, Changsha, Hunan 410001, China

ARTICLE INFO

Keywords:
Sulfite
Activation methods
Advanced oxidation process
Advanced reduction process
Water treatment

ABSTRACT

Sulfite has attracted increasing attention as a precursor to produce highly reactive species to eliminate pollutants from water due to the merits of abundant sources, low cost and low eco-toxicity. The systems can be cataloged into advanced oxidation processes (AOPs) and advanced reduction processes (ARPs) according to the redox characteristics of reactive species produced by sulfite activation, thus broadening the scope of application. Herein, this critical review provides a fundamental aspect of sulfite-based AOPs/ARPs and their state-of-the-art developments in water purification. Oxidative species can be generated via sulfite activation using homogenous or heterogeneous transition metals (e.g., zero-valent metals, metal oxides, metal sulfides and supported metals), and the corresponding activation mechanisms are discussed in detail. More importantly, sulfite can be activated by UV irradiation to produce reductive species (including hydrated electrons, hydrogen radicals and sulfite radicals), with emphasis on their chemical properties, reaction mechanisms and improved strategies. In addition, the key factors affecting the removal performance of sulfite-based AOPs/ARPs are also highlighted, such as dissolved oxygen, pH, sulfite concentration and water constituents. The reactive species produced are identified in quantitative and qualitative ways, and their roles in destructing pollutants are analyzed. Furthermore, key knowledge gaps are identified and future research directions are proposed to address the application challenges. This review article aims to advance our understanding and consequent applications of sulfite-based AOPs/ARPs in water treatment.

1. Introduction

With the rapid development of urbanization and industrialization, problems such as water shortage and water pollution have become increasingly prominent. Various compounds are released into the aquatic environment at relatively high exposure concentrations, posing a potential threat to humans and ecosystems [1,2]. Especially, contaminants of emerging concern (CECs) including pharmaceuticals, personal care products, hormones, and antibiotics have been frequently detected in effluents of wastewater treatment plants (WWTPs) at trace levels (ng/L to μg/L), indicating that WWTPs have become a major release point of CECs [3–5]. Consequently, the development of cost-effective and high-performance approaches for water purification has become a priority [6–9].

Over the past two decades, sulfate radicals-based advanced oxidation processes ($SO_4^{\bullet-}$-based AOPs) have attracted widespread attention and have been demonstrated to be an effective technology for removing a wide range of contaminants [10–14]. Compared with hydroxyl radicals (•OH), $SO_4^{\bullet-}$ have higher oxidation and mineralization abilities and selectivity for organics degradation [15–19]. Most commonly, the generation of $SO_4^{\bullet-}$ can be realized via activation of persulfate [11,20–22]. Various strategies have been developed for activating persulfate to produce $SO_4^{\bullet-}$, including radiation, ultrasound, heat, alkaline, transition metals, and carbonaceous materials [20,23–26]. However, the cost of persulfate is relatively high and the residual persulfate in the treated system has an acute toxicity due to durable stability (Table 1), which

---

[*] Corresponding author at: School of Environmental Science and Engineering, Guangdong University of Petrochemical Technology, Maoming, Guangdong 525000, China.

E-mail address: yangc@hnu.edu.cn (C. Yang).

https://doi.org/10.1016/j.cej.2021.128872
Received 31 October 2020; Received in revised form 30 January 2021; Accepted 3 February 2021

Table 1
Comparisons of the properties of precursors and their activation processes.

Properties	Sulfite	Persulfate	Peroxymonosulfate
CAS number	7757-83-7	7727-21-1	37222-66-5
Formula	Na_2SO_3	$K_2S_2O_8$	$H_3K_5O_{18}S_4$
Molecule weight (g/mol)	126.04	270.31	614.74
Solubility in water (20 °C) (g/L)	126	549	250
Toxicity (LD_{50}; Oral, Rat) (mg/kg)	3560	825	2000
Price ($ per kg)	0.35	1.83	3.11
Redox potential (V)	−0.93	2.01	1.82
Comparison of activation process	Sulfite activation		Persulfate/peroxymonosulfate activation
Disadvantages	1. Little research in other environmental media, besides water matrix2. Low activation efficiency		1. High price and eco-toxicity of persulfates2. Low utilization efficiency of persulfates due to its direct oxidation with water matrix
Advantages	1. Achieving reduction and dehalogenation of pollutants, besides oxidation2. Low price, eco-toxicity, and abundant source of sulfite		1. High degradation efficiency and reactive species yield2. Various activation methods3. Diverse activation mechanisms, including radical and non-radical pathways, suiting for various environmental condition and matrix
Challenges	Seen in Section 6		1. Uncertainty of toxicity in degradation2. Metal leaching and reusability3. Practice application

may hamper its widespread use to some extent. Therefore, new attempts should be made to seek greener and more cost-effective $SO_4^{\bullet -}$ precursors.

To this end, sulfite has emerged as a promising alternative to persulfate [27], and comparisons of their activation process are summarized in Table 1. In addition to commercial purchases, considering that sulfur dioxide (SO_2) is a major air pollutant and sulfite is a common industrial by-product, its use is expected to achieve the purpose of waste control by waste. Initially, some researchers discovered that the Fe(III)-catalyzed autoxidation of SO_2 in tropospheric clouds was crucial to the formation of acid rain [28–32]. Subsequently, Lee and Rochelle [33] investigated the degradation of organic acid conjugated with sulfite oxidation during flue gas desulfurization processes. They stated that certain transition metals (e.g., Fe, Ni, Co and Cu) could enhance the oxidative degradation rate and $SO_4^{\bullet -}$ were generated as the primary species causing degradation. Moreover, the residual sulfite in water can be removed by aeration, leading to the formation of non-toxic sulfate [34,35]. Consequently, $SO_4^{\bullet -}$ generated by sulfite activation are progressively applied to eliminate pollutants in water. More excitingly, sulfite-based AOPs are also suitable for treating bromine-containing organic wastewater, without the formation of bromate [36,37]. Zhou et al. [38] summarized $SO_4^{\bullet -}$-based AOPs for water purification via homogenous transition metal-catalyzed auto-oxidation of sulfite. However, metal ions in solution have some inherent drawbacks, such as narrow pH working range, difficulties in recovery and potential secondary pollution. Aiming at these issues, heterogeneous catalysts have been recently exploited to activate sulfite, such as zero-valent metals [39], metal oxides [40] supported metals [41] and bimetallic oxides [42,43]. Besides, a novel visible light-driven photocatalysis is used to activate sulfite, which is expected to expand the utilization efficiency of sunlight [36,44].

In addition, sulfite has a strong ultraviolet (UV) absorption. Under UV irradiation, sulfite can be stimulated to produce reductive species including sulfite radicals ($SO_3^{\bullet -}$), hydrated electrons (e_{aq}^-) and hydrogen radicals (•H), which essentially differs from UV/persulfate system that produces the dominant $SO_4^{\bullet -}$ [45]. Based on those powerful reductive species (Table 2), the combination of sulfite and UV irradiation is considered as a promising advanced reduction processes (ARPs) for the destruction of contaminants. For example, UV/sulfite process is effective in removing halogenated organic compounds [46,47], heavy metals [48–50], bromate [51] and perchlorate [52]. More interestingly, e_{aq}^- generated by UV/sulfite process can not only effectively degrade per- and polyfluoroalkyl substances, but also cleave the carbon–fluorine bond to achieve efficient defluorination, which is difficult for $SO_4^{\bullet -}$-based AOPs [45,53,54]. To improve the yield of e_{aq}^- in UV/sulfite process, some chemical reagents including iodide [46,55] and bismuth oxyiodide [56] are added.

Therefore, employing sulfite as a precursor is fascinating and various activation methods can be customized to achieve oxidative or reductive removal of contaminants. Nevertheless, the systematic review regarding sulfite as a precursor to drive AOPs/ARPs has not been reported yet. To fulfill this knowledge gap, the present review provides the latest progresses on sulfite-based AOPs/ARPs for the abatement of contaminants in water, with emphasis on the methods and mechanisms of sulfite activation, key factors influencing the removal performance and detection technology for the reactive species. Furthermore, key knowledge gaps are identified and future research directions are proposed.

2. Overview of recent progresses in sulfite-based AOPs

For sulfite-based ARPs/AOPs, it is highly dependent on activation methods. So far, metal activation methods have been reported to induce the generation of oxidative radicals such as $SO_4^{\bullet -}$, $SO_5^{\bullet -}$ and •OH (Fig. 1), while UV-activated method has been shown to produce reductive species ($SO_3^{\bullet -}$, e_{aq}^- and •H). It is significant to understand and control the fundamental activation process, since the degradation of contaminants is greatly affected by the types of reactive species generated.

2.1. Homogenous transition metals for sulfite activation

2.1.1. Iron-based activators

The Fe-catalyzed SO_2 oxidation by oxygen (Fe-SO_2-O_2) has always been an important research subject in atmospheric chemistry because of its significance in sulfur transformation, aerosol nucleation and acid precipitation [57]. Despite the quite complicated reactions of Fe-SO_2-O_2 system, free radical chain reactions have been proposed as a widely accepted mechanism [58,59]. Due to the low-cost and environmental-friendliness of Fe-based species, they have been used to activate sulfite for the remediation of contaminated water [27,60–62].

Both Fe(II) and Fe(III) can activate sulfite to produce $SO_4^{\bullet -}$, as described in Eqs.(1–10) [38,60]. More specifically, the initiation step is to form Fe(III)-sulfito complexes, which can spontaneously decompose into $SO_3^{\bullet -}$ and Fe(II) (Eqs. (1, 2)) [63]. The generated $SO_3^{\bullet -}$ react rapidly with O_2 to produce $SO_5^{\bullet -}$ (Eq. (3)), which is a diffusion-controlled reaction [64]. Subsequently, a series of chain reactions are initiated, resulting in the generation of $SO_4^{\bullet -}$ (Eqs. (4–10)) [33,65]. There are two pathways for generating $SO_4^{\bullet -}$, among which the reaction of $SO_5^{\bullet -}$ and HSO_3^- contributes more. Furthermore, $SO_4^{\bullet -}$ can be converted to •OH by reaction with water (Eq. (11)). Zhou et al. [38] speculated that most metal ions existed as metal-sulfite complexes in the presence of excess

Table 2
The common reactive species involved in the activated sulfite system.

Reactive species	Redox potentials (V)	References
$SO_4^{\bullet -}$	2.5–3.1	[196]
•OH	2.8	
$SO_5^{\bullet -}$	0.81–1.1	
e_{aq}^-	−2.9	[164]
•H	−2.3	
$SO_3^{\bullet -}$	0.63	

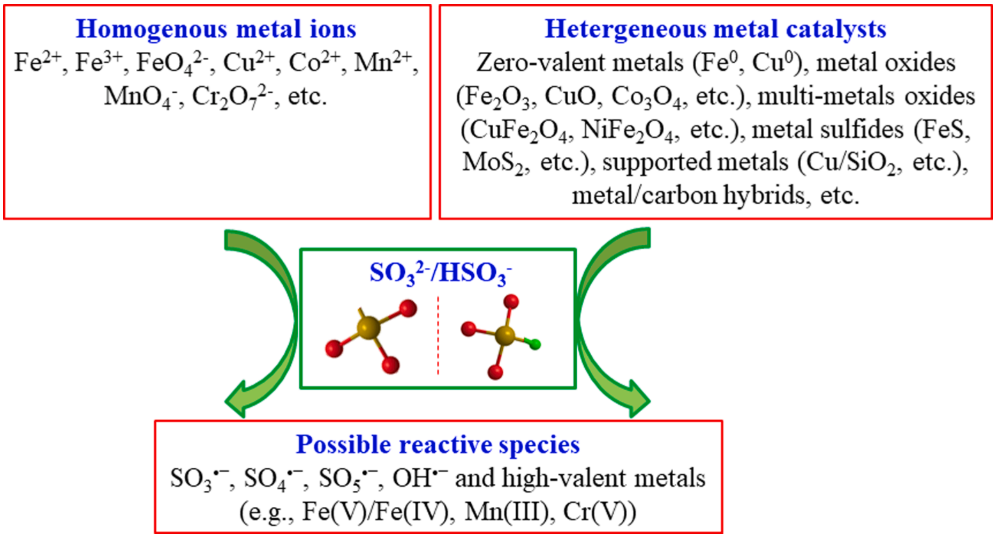

Fig. 1. The activation of sulfite by homogenous and heterogeneous metal catalysts.

sulfite, rather than as free metal ions with a reduced state. It is noteworthy that the contributions of each oxysulfur radicals on contaminants degradation varies significantly in the Fe(III)/sulfite system (Table 3). In particular, the contribution of $SO_5^{\bullet-}$ in the Fe(III)/sulfite system is related to the types of target pollutants, ranging from 10.3% to 60.0%, even exceeding that of $SO_4^{\bullet-}$. Despite the low oxidative capability of $SO_5^{\bullet-}$ with a low redox potential (Table 2), its generation rate is much higher than conversion rate, which may result in the concentration of remaining $SO_5^{\bullet-}$ being sufficient to oxidize some pollutants. Especially, $SO_5^{\bullet-}$ can show moderate reactivity toward aromatic amines, hydroquinone and other hydroxyphenols via one-electron redox reactions [66]. To date, the role of $SO_5^{\bullet-}$ in most of the oxidation processes that may be involved, including peroxomonosulfate activation, is unclear, so more attention is needed. Because the formation of $SO_5^{\bullet-}$ is an oxygen-consuming process, the presence of dissolved oxygen and its concentration played a key role in regulating the conversion between oxysulfur radicals. In future studies, experiments should be performed on quantitatively controlling the concentration of dissolved oxygen to better understand the exact role of oxysulfur radicals in the Fe(III)/sulfite system.

$$Fe^{3+} + HSO_3^- \leftrightarrow FeSO_3^+ + H^+ (k = 600) \quad (1)$$

$$FeSO_3^+ \leftrightarrow SO_3^{\cdot-} + Fe^{2+} (k = 0.19 s^{-1}) \quad (2)$$

$$SO_3^{\cdot-} + O_2 \rightarrow SO_5^{\cdot-} (k = (1.0 - 2.5) \times 10^9 M^{-1} s^{-1}) \quad (3)$$

$$SO_5^{\cdot-} + HSO_3^- \rightarrow HSO_5^- + SO_3^{\cdot-} (k = 8.6 \times 10^3 - 3.0 \times 10^5 M^{-1} s^{-1}) \quad (4)$$

$$SO_5^{\cdot-} + HSO_3^- \rightarrow SO_4^{2-} + SO_4^{\cdot-} + H^+ (k = 3.6 \times 10^3 - 3.0 \times 10^5 M^{-1} s^{-1}) \quad (5)$$

$$HSO_5^- + HSO_3^- \rightarrow 2SO_4^{2-} + 2H^+ \ (k = 1.0 \times 10^3 M^{-1} s^{-1}) \quad (6)$$

$$SO_4^{\cdot-} + HSO_3^- \rightarrow SO_4^{2-} + SO_3^{\cdot-} + H^+ (k > 2.0 \times 10^9 M^{-1} s^{-1}) \quad (7)$$

$$Fe^{2+} + SO_5^{\cdot-} + H^+ \rightarrow Fe^{3+} + HSO_5^- (k = (4.3 \pm 2.4) \times 10^7 M^{-1} s^{-1}) \quad (8)$$

$$Fe^{2+} + HSO_5^- \rightarrow Fe^{3+} + SO_4^{\cdot-} + OH^- (k = 1.0 \times 10^3 M^{-1} s^{-1}) \quad (9)$$

$$Fe^{2+} + SO_4^{\cdot-} \rightarrow Fe^{3+} + SO_4^{2-} (k = 8.6 \times 10^8 M^{-1} s^{-1}) \quad (10)$$

$$SO_4^{\cdot-} + H_2O \rightarrow SO_4^{2-} + \cdot OH + H^+ (k = (0.1 - 1.0) \times 10^4 M^{-1} s^{-1}) \quad (11)$$

The production efficiency of $SO_4^{\bullet-}$ depends largely on the redox cycle of Fe(II)/Fe(III) [68,69]. Interestingly, when Fe(II) or Fe(III) is used as sulfite activator, the degradation efficiency of pollutants is almost comparable [27,70]. This phenomenon can be explained as the decomposition of Fe(III)-sulfto complexes is a rate-determining step in the generation of $SO_4^{\bullet-}$ [71,72]. Additionally, Fe(III)/sulfite process only works effectively at pH < 4.0, because Fe(III) is prone to precipitate at pH > 4.0 [73]. To broaden the pH working range and degradation efficiency of the system, photo irradiation (e.g., UV light, visible light, UV–Vis light and sunlight) is introduced into the Fe(III)/sulfite process [70,73–75]. For example, the presence of UV irradiation greatly enhances the degradation efficiency of 2,4,6-trichlirophenol from 15% to 90% at pH 4.0 [73]. The authors explained that the introduction of UV irradiation can accelerate the decomposition of Fe(III)-sulfto complexes to generate $SO_4^{\bullet-}$ as well as the transformation of Fe(III)-sulfito to Fe(III)-hydroxo complexes for •OH generation, because Fe(III)-sulfito complexes have a strong and wide light absorption range (290–575 nm) [76].

In addition, high-valent iron species (ferrate(VI), Fe(VI)) have attracted much attention due to the following advantages. (1) Fe(VI) itself can function as oxidants, coagulants, adsorbents and disinfectants [77–79]. (2) A broad spectrum of contaminants can be rapidly degraded within 30 s in the Fe(VI)/sulfite process [80]. (3) Fe(VI)/sulfite system has a wider pH working range than Fe(III)/sulfite system [81]. Acosta-Rangel et al. [82] evaluated the effectiveness of iron species with different oxidation states on sulfite activation through the degradation of sulfamethazine. The results suggested that the presence of iron species could accelerate the degradation and its effectiveness followed Fe(VI) > Fe(0) > Fe(II) > Fe(III). However, the reaction mechanism for Fe(VI)/sulfite process is still unclear and under debate. For example, some researchers proposed that the reaction of Fe(VI) and sulfite could produce more $SO_3^{\bullet-}$ through one-electron transfer (Eq. (12)), and then participated in the generation of dominant $SO_4^{\bullet-}$ via Eqs. (3, 5) [83–85]. Multi-oxidizing species (including (Fe(V)/Fe(IV)), $SO_3^{\bullet-}$, $SO_4^{\bullet-}$ and •OH) may coexist in the Fe(VI)/sulfite process [86]. In addition, Shao et al. [87] investigated the performance and mechanism of Fe(VI)/sulfite process by using sparingly soluble $CaSO_3$ as the slow release source of SO_3^{2-}. The result verified that Fe(V)/Fe(IV) were the main oxidants responsible for degradation, as described in Eqs. (12–17). Feng et al. [80] also speculated Fe(V) as primary reactive species, which caused an accelerated oxidation of trimethoprim. As reported, Fe(V) are more reactive than Fe (VI) by 3–5 orders of magnitude [88]. Moreover, the molar ratio of sulfite to Fe(VI) is a key factor in regulating the conversion of reactive species [89]. Specifically, Fe(V) will become the main oxidant when the molar ratio is in the range of 0.1–0.3, and increasing the molar ratio will lead to the coexistence of Fe(V) and $SO_4^{\bullet-}$/•OH. Once the molar ratio is

Table 3
Summary of homogenous transition metals-activated sulfite for the abatement of contaminants.

Activators	Contaminants	Reaction condition	Reactive species	Refs.
Fe(II)	Orange II	[Fe(II)] = 100 μM, [sulfite] = 1.0 mM, [Cont] = 10 mg/L, pH 4.0, about 80% in 120 min	$SO_4^{\bullet -}$ (74.8%), $SO_5^{\bullet -}$ (11.3%) and•OH (13.9%)	[27]
Fe(III)	Carbamazepine	[Fe(III)] = 100 μM, [sulfite] = 0.5 mM, [Cont] = 5.0 μM, pH 4.0–6.0, 88–90% in 60 min	$SO_4^{\bullet -}$ (65.75%), $SO_5^{\bullet -}$ (10.96%) and•OH (23.29%)	[60]
Fe(III)	Bisphenol A	[Fe(III)] = 100 μM, [sulfite] = 1.0 mM, [Cont] = 1.0 mg/L, pH 6.0, about 70% in 60 min	$SO_4^{\bullet -}$ (47.7%), $SO_5^{\bullet -}$ (37.3%) and•OH (15.0%)	[70]
Fe(III)	Aniline	[Fe(III)] = 100 μM, [sulfite] = 1.0 mM, [Cont] = 10.0 μM, pH 4.0, about 70% in 80 min	$SO_4^{\bullet -}$ (35.9 ± 1.0%), $SO_5^{\bullet -}$ (~60.0%) and•OH (2.5 ± 4.9%)	[67]
Fe(III)	Tetrabromobisphenol A	[Fe(III)] = 40 μM, [sulfite] = 0.4 mM, [Cont] = 10.0 μM, pH 4.0, about 73.4% in 30 min	$SO_4^{\bullet -}$ and•OH (main)	[212]
Fe (VI)	N,N-diethyl-3-toluamide	[Fe(VI)] = 100 μM, [sulfite] = 0.4 mM, [Cont] = 10.0 μM, pH 8.0, about 78% in 10 s	$SO_4^{\bullet -}$	[83]
Fe(VI)	Trimethoprim	[Fe(VI)] = 100 μM, [sulfite] = 0.4 mM, [Cont] = 5.0 μM, pH 8.0, ~100% in 30 s	Fe(V)	[80]
Fe(VI)	Phenol, methyl blue, rhodamine B, ciprofloxacin,	[Fe(VI)] = 50 μM, [sulfite] = 0.25 mM, [Cont] = 5.0 μM, pH 9.0, greater than 90% in 30 s	$SO_4^{\bullet -}$ and •OH	[81]
Fe(VI)	Trimethoprim	[Fe(VI)] = 100 μM, [sulfite] = 0.15–0.4 mM, [Cont] = 20.0 μM, pH 9.0, about 45% in 15 s	Fe(V)/Fe(IV), $SO_4^{\bullet -}$, $SO_3^{\bullet -}$ and•OH	[86]
Co(II)	Iohexol	[Co(II)] = 10 μM, [sulfite] = 0.5 mM, [Cont] = 10.0 μM, pH 8.0, almost 100% in 20 min	$SO_4^{\bullet -}$ (main) and •OH	[91]
Co(II)	Paracetamol	[Co(II)] = 100 μM, [sulfite] = 1.0 mM, [Cont] = 10.0 μM, pH 8.0, almost 82% in 10 min	$SO_4^{\bullet -}$ (main) and $SO_5^{\bullet -}$ (possible)	[92]
Cu(II)	Iohexol	[Cu(II)] = 10 μM, [sulfite] = 0.5 mM, [Cont] = 10.0 μM, pH 8.0, almost 100% in 40 min	$SO_4^{\bullet -}$ and •OH	[91]
Cu(II)	Glyphosate	[Cu(II)] = 25 μM, [sulfite] = 0.25 mM, [Cont] = 6.0 μM, pH 9.0, about 81.0% in 30 min	$SO_4^{\bullet -}$ (53.0%) and•OH (47.0%)	[94]
Mn(II)	Atrazine	[Mn(II)] = [Fe (II)] = 10 μM, [Cont] = 6.0 μM, [sulfite] = 0.5 mM, pH 6.0, 98.31% in 180 s	Mn(III)	[97]
Mn(VII)	Arsanilic acid	[Mn(VII)] = 50 μM, [sulfite] = 0.25 mM, [Cont] = 5.0 μM, pH 5.0, about 71.0% in 300 s	Mn(III), $SO_4^{\bullet -}$ (main) and •OH	[103]
Cr(VI)	As(III)	[Cr(VI)] = 50 μM, [sulfite] = 0.4 mM, [Cont] = 50.0 μM, pH 3.5, 64.0% oxidation in 60 min	$SO_4^{\bullet -}$ and •OH	[107]
Cr(VI)	Orange II	[Cr(VI)] = 100 μM, [sulfite] = 0.55 mM, [Cont] = 29.0 μM, pH 3.0, 57.7% in 30 min	$SO_4^{\bullet -}$ + $SO_5^{\bullet -}$ (72.5%) and•OH (21.7%)	[108]
Cr(VI)	4-chlorophenol	[Cr(VI)] = 100 μM, [sulfite] = 1.0 mM, [Cont] = 5.0 μM, pH 4.0, 100% in 450 s	$SO_4^{\bullet -}$	[111]
Cr(VI)	Methyl phenyl sulfoxide	[Cr(VI)] = 100 μM, [sulfite] = 0.5 mM, [Cont] = 20.0 μM, pH 4.0, over 80% in 20 min	Cr(V)	[109]

beyond 1.5, $SO_4^{\bullet -}$/•OH will become exclusive oxidants. Therefore, the reaction conditions (such as Fe(VI)/PMS molar ratio, pH and the concentration of dissolved oxygen) should be strictly controlled to further explore the reaction mechanisms of Fe(VI)/sulfite system. Meanwhile, sulfite activation also changes the features of Fe(VI) resultant particles, making them less magnetic, less crystalline and more polydisperse [90].

$$Fe(VI) + SO_3^{2-} \rightarrow Fe(V) + SO_3^{\bullet -} \tag{12}$$

$$Fe(VI) + SO_3^{\bullet -} \rightarrow Fe(V) + SO_3 \tag{13}$$

$$Fe(V) + SO_3^{\bullet -} \rightarrow Fe(IV) + SO_3 \tag{14}$$

$$Fe(V) + H_2O + H^+ \rightarrow Fe(OH)_3 + H_2O_2 \tag{15}$$

$$2Fe(V) \rightarrow 1/3H_2O_2 + 2Fe(III) + 1/3O_2 \tag{16}$$

$$Fe(V) + Fe(OH)_2 + H_2O \rightarrow Fe(VI) + Fe(OH)_3 \tag{17}$$

2.1.2. *Cobalt-based activators*

In comparison with Fe(III) ions ($pH < 4.0$), Co(II) ions can effectively activate sulfite to degrade organic pollutants under neutral and alkaline condition [91,92]. This is due to the fact that Co(II) ions can form Co(II)–OH complexes by reacting with H_2O under alkaline conditions (Eq. (18)) [91]. Co(II)–OH complexes are more reactive toward SO_3^{2-} than HSO_3^-, thus leading to the formation of Co(II)-sulfite complexes (Eq. (19)) [34]. When dissolved oxygen is present, Co(II)-sulfite complexes can be transformed into $CoSO_3^+$ and then reacts with sulfite to produce $SO_3^{\bullet -}$ (Eqs. (20, 21)) [93]. Furthermore, $SO_3^{\bullet -}$ can be oxidized by O_2 to $SO_5^{\bullet -}$ (Eq. (3)), which can further react with SO_3^{2-}/HSO_3^- to produce $SO_4^{\bullet -}$/$SO_3^{\bullet -}$ at different reaction rates (Eqs. (4, 5, 22, 23)). The detailed mechanism has been proposed by Yuan et al. [92].

$$\mathrm{Co}(II) + H_2O \rightarrow \mathrm{Co}(II) - OH(alkaline) \tag{18}$$

$$\mathrm{Co}(II) - OH + SO_3^{2-} \rightarrow \mathrm{Co}(II) - SO_3 + H_2O \tag{19}$$

$$\mathrm{Co}(II) - SO_3 + O_2 \rightarrow \mathrm{Co}(II) - SO_3^+ \tag{20}$$

$$\mathrm{Co}(II) - SO_3^+ + SO_3^{2-} \rightarrow \mathrm{Co}(II) - SO_3 + SO_3^{\bullet -} \tag{21}$$

$$SO_5^{\bullet -} + SO_3^{2-} \rightarrow HSO_4^- + SO_4^{\bullet -}(k = (5.5 - 9.0) \times 10^6 M^{-1} s^{-1}) \tag{22}$$

$$SO_5^{\bullet -} + SO_3^{2-} \rightarrow HSO_5^- + SO_3^{\bullet -}(k = (3.0 - 3.8) \times 10^6 M^{-1} s^{-1}) \tag{23}$$

2.1.3. *Copper-based activators*

Similar to Co(II) ions, Cu(II) ions also exhibit effective sulfite activation over a wide pH range [91]. Moreover, Cu(II)/Cu(I) cycle is responsible for generating $SO_3^{\bullet -}$ in the Cu(II)/sulfite system (Eqs. (24–26)) [91,94]. Subsequently, the generated $SO_3^{\bullet -}$ are involved in the chain reactions, resulting in the formation of $SO_4^{\bullet -}$ and •OH.

$$Cu(II) + SO_3^{2-} \rightarrow Cu(II) - SO_3^{2-} \tag{24}$$

$$Cu(II) - SO_3^{2-} + O_2 \rightarrow Cu(I) - SO_3^{2-} + O_2^- \tag{25}$$

$$Cu(I) - SO_3^{2-} \rightarrow Cu(II) + SO_3^{\bullet -} \tag{26}$$

2.1.4. *Manganese-based activators*

Mn(II)/sulfite process is ineffective in dye removal and bacterial inactivation as a result of narrow pH working range, and its reaction mechanism is analogous to Fe(II)/sulfite process [95]. To improve the oxidation ability of Mn(II)/sulfite process under neutral conditions, several strategies have been proposed, such as electrolysis assistance [96] and Fe(II) addition [97]. The main difference between the two activation strategies lies in the reactive species and reaction mechanisms involved. $SO_4^{\bullet -}$ are the main reactive species in the electro/Mn(II)/sulfite system and their generation is promoted by the anode reaction, including the oxygen from water electrolysis, direct sulfite oxidation and local acidic pH [96]. In contrast, highly reactive Mn(III) is recognized as the major oxidant rather than $SO_4^{\bullet -}$ in the Fe(II)/Mn(II)/sulfite system [97]. The generation of Mn(III) is attributed to the reaction between Mn (II) and $SO_5^{\bullet -}$ supplied by the Fe(II)/sulfite system (Eqs. (27, 28)) [98]. Moreover, the system is also an effective approach to remove Mn(II) from water via adsorption and oxidation [99]. In addition, Mn(III) can be produced by Mn(VII)/sulfite system, resulting in the rapid oxidation of various contaminants [84,100–102]. However, recent studies have showed that Mn intermediates, $SO_4^{\bullet -}$ and •OH are produced, among which $SO_4^{\bullet -}$ are the major contributor [103,104]. Comparing these studies, the differences in reaction mechanism in Mn(VII)/sulfite system are due to the presence of dissolved oxygen in the solution. The generated Mn(III) can produce the first radical $SO_3^{\bullet -}$ via Eq. (28), which can further evolve into secondary radicals (including $SO_4^{\bullet -}$, $SO_5^{\bullet -}$ and •OH) in the presence of dissolved oxygen. Meanwhile, Mn(III) itself is unstable, and can be quickly and spontaneously decomposed into MnO_2 and Mn(II) [100]. In view of this, when exploring the reaction mechanism of the system, the reaction conditions should be declared under anaerobic or aerobic environments.

$$Mn(II) + SO_5^{\bullet -} + H^+ \rightarrow Mn(III) + HSO_5^-(k \approx 10^8 M^{-1} s^{-1}, pH = 1 - 4) \tag{27}$$

$$Mn(III) + MnHSO_3^+ \rightarrow 2Mn(II) + SO_3^{\bullet -} + H^+(k = 1.3 \pm 0.6 \times 10^6 M^{-1} s^{-1}, pH = 2.4) \tag{28}$$

2.1.5. *Chromium-based activators*

Hexavalent chromium (Cr(VI)) is frequently detected at relative high concentrations in the environment due to its wide use in industrial processes [105,106]. Moreover, Cr(VI) has been registered as a priority pollutant by the U.S. Environmental Protection Agency owing to its toxicity and carcinogenicity. Generally, reducing Cr(VI) to Cr(III) with sulfite is a feasible approach to reduce its toxicity and mobility. More excitingly, this system can also produce highly reactive species to remove other contaminants, e.g., As(III) [107], phenolic-, amino-, and dye compounds [108,109]. Therefore, Cr(VI)/sulfite system is a promising strategy to achieve a win–win goal for environmental remediation. The mechanism of Cr(VI) reduction by sulfite is that the continuous condensation of Cr(VI) with sulfite leads to the formation of activated complexes ($CrSO_6^{2-}$ and $CrO_2(SO_3)_2^{2-}$) (Eqs. (29, 30)). Subsequently, $CrO_2(SO_3)_2^{2-}$ can be spontaneously decomposed into $SO_3^{\bullet -}$ via an intermolecular electron-transfer reaction (Eq. (31)) [110]. The generated $SO_3^{\bullet -}$ are further involved in the formation of $SO_4^{\bullet -}$, $SO_5^{\bullet -}$ and •OH, of which $SO_4^{\bullet -}$ are the key oxidants responsible for contaminants removal [108,111]. Besides $SO_4^{\bullet -}$, recent studies have also identified the non-negligible role of high-valent Cr intermediates (Cr(V)/Cr(IV)) during the Cr(VI)/sulfite system (Eqs. (32–34)) [109,112]. For example, Dong et al. [109] revealed that both Cr(V) and $SO_4^{\bullet -}$ were the main reactive species contributing to the degradation of organic contaminants under oxygenated conditions and their relative contributions largely depended on the chemical structures of contaminants and solution pH. In addition, the addition of citric acid or thiocyanate into Cr(VI)/sulfite system can enhance the reduction of Cr(VI) and decrease the consumption of sulfite [113,114].

$$HCrO_4^- + HSO_3^- \rightarrow CrSO_6^{2-} + H_2O \tag{29}$$

$$CrSO_6^{2-} + H^+ + HSO_3^- \rightarrow CrO_2(SO_3)_2^{2-} + H_2O \tag{30}$$

$$CrO_2(SO_3)_2^{2-} + 2H^+ + 4H_2O \rightarrow SO_4Cr(H_2O)_5^+ + SO_3^{\bullet -} \tag{31}$$

$$Cr(VI) + HSO_3^- \rightarrow Cr(V) + SO_3^{\bullet -} + H^+(k < 8.3 \times 10^6 M^{-1} s^{-1}) \tag{32}$$

$$Cr(V) + HSO_3^- \rightarrow Cr(IV) + SO_3^{\bullet -} + H^+(k = 8.3 \times 10^6 M^{-1} s^{-1}) \tag{33}$$

$$Cr(IV) + HSO_3^- \rightarrow Cr(III) + SO_3^{\bullet -} + H^+(k < 2.38 \times 10^5 M^{-1} s^{-1}) \tag{34}$$

Some researchers compared the performance of transition metals ions on sulfite activation. For example, sulfite can be rapidly activated by metals ions, generating free radicals that can cause DNA damage, and the effectiveness is as follows: Fe(III) > Co(II) > Cu(II) > Cr(VI) > Mn(II) [115]. Chen et al. [95] reported that homogenous metal/sulfite systems could effectively kill *Escherichia coli* via $SO_4^{\bullet -}$ oxidation and the inactivation rate followed Cu(II) > Fe(II) > Co(II) > Mn(II). Zhao et al. [91]

found that the activity order of metal ions for sulfite activation to degrade iohexol at pH 8.0 was Co(II) > Cu(II) > Mn(II) > Fe(II) > Fe(III) ≈ Ce(III) ≈ Ag(I). Of note, the performance of metal ions is not necessarily related to their redox potential.

2.2. Heterogeneous metal catalysts for sulfite activation

Despite some progress has been made in homogenous activated systems, the toxicity of transition metals ions and potential secondary treatment costs may impede large-scale applications. Moreover, the activity of transition metals ions (e.g., Fe(II), Fe(III), Mn(II) and Cr(VI)) for sulfite activation is highly dependent on acid pH. In view of this, heterogeneous catalysts, which are characterized as excellent reactivity and stability, easy separation and low metal leaching, have been developed to activate sulfite (Table 4, Fig. 1). So far, the heterogeneous catalysts involved in sulfite activation mainly include zero-valent metals, metal oxides, metal sulfides and their supported metals.

2.2.1. Zero-valent metals

Zero-valent metals, have been widely applied to the remediation of contaminants in soils, groundwater and surface water because of high reactivity [23,116–118]. Xie et al. [39] established a novel AOPs system through the activation of sulfite using zero-valent iron. Zero-valent iron can slowly and continuously release Fe(II) ions, thus easing the consumption of $SO_4^{\bullet-}$ by excess Fe(II) and improving the removal of contaminants [119]. Moreover, the performance of zero-valent iron on sulfite activation is superior to that of Fe(II) and Fe(III) [39,82]. Differently, Du et al. [120] showed that •OH instead of $SO_4^{\bullet-}$ are main radicals responsible for sulfamethoxazole degradation. In addition, the reactivity of zero-valent iron can be further enhanced. For example, $Fe@Fe_2O_3$ core shell nanoparticles obtained by aging of zero-valent iron can cause Orange II to degrade by more than 99% at pH 3.0 within 30 s [121]. The authors deeply confirmed that transferring electrons from Fe core to Fe_2O_3 shell promoted Fe(III)/Fe(II) cycle, thereby accelerating the generation of $SO_4^{\bullet-}$/•OH. Compared to zero-valent iron, the incorporation of mesoporous carbon can enhance the activation efficiency of sulfite [122]. Furthermore, the introduction of simulated sunlight into zero-valent iron/sulfite system can enhance the decomposition of $FeSO_3^+$ to produce more $SO_3^{\bullet-}$ and $SO_4^{\bullet-}$ [36]. Besides, zero-valent copper can activate sulfite to generate $SO_4^{\bullet-}$ and its reactivity outperforms zero-valent iron [123].

2.2.2. Metal oxides

Metal oxides can be prepared to activate sulfite for the destruction of organic contaminants. For example, Mei et al. [124] found that Fe_2O_3 was capable of activating sulfite to achieve efficient degradation of Orange II without Fe leaching. This observation indicated that sulfite activation occurred at the catalyst surface rather than free Fe(III) ions in aqueous solution, and the activation mechanism was described in Eqs. (3, 5, 35, 36). Wu et al. [40] showed that copper oxides including Cu_2O and CuO had excellent catalytic activity toward sulfite activation, and the reactivity of CuO was higher. Note that the Cu leaching amount from CuO/sulfite system is relatively higher, accounting for 0.72% of the total CuO, which can be explained by the strong inner-sphere interaction between sulfite and CuO. In addition, sulfite can be effectively activated by cobalt oxides (e.g., Co_3O_4 and CoO) [34,40]. Interestingly, Zhu et al.

Table 4
Summary of heterogeneous catalysts-activated sulfite for the abatement of contaminants.

Activators	Synthetic methods	Contaminants	Reaction conditions	Reactive species	Refs.
Zero-valent iron	Commercial use	Reactive brilliant red	[Cata] = 0.2 mM, [sulfite] = 1.0 mM, [Cont] = 20 mg/L, pH 6.0, 69.5% in 90 min	$SO_4^{\bullet-}$ (main) and •OH	[39]
Zero-valent iron	Commercial use	Sulfamethoxazole	[Cata] = 1.0 mM, [sulfite] = 1.0 mM, [Cont] = 5.0 μM, pH 4.0, about 80% in 60 min	$SO_4^{\bullet-}$ and •OH (main)	[120]
Core shell $Fe@Fe_2O_3$	Borohydride reduction and aging	Orange II	[Cata] = 1.0 g/L, [sulfite] = 50 mM, [Cont] = 200.0 μM, pH 3.0, 99% in 5 min	$SO_4^{\bullet-}$ and•OH	[121]
Zero-valent iron/mesoporous carbon	Soft template method and carbonization	Reactive brilliant red	[Cata] = 0.3 g/L, [sulfite] = 5.0 mM, [Cont] = 20 mg/L, pH 6.0, about 95% in 60 min	$SO_4^{\bullet-}$ and •OH	[122]
Zero-valent copper	Commercial use	Iohexol and atrazine	[Cata] = 0.5 g/L, [sulfite] = 0.5 mM, [Cont] = 10.0 μM, pH 8.0, over 90% in 30 min	$SO_4^{\bullet-}$	[123]
Fe_2O_3	Precipitation and calcination	Orange II	[Cata] = 0.25 g/L, [sulfite] = 1.0 mM, [Cont] = 20.0 μM, pH 8–10, over 90% in 20 min	$SO_4^{\bullet-}$ and •OH	[124]
$LiCoO_2$	Calcination	Rhodamine B	[Cata] = 4.0 g/L, [sulfite] = 1.0 g/L, [Cont] = 5.0 mg/L, pH 8–10, ~ 100% in 20 min	$SO_3^{\bullet-}$	[125]
Copper oxides	Commercial use	Iohexol	[Cata] = 0.5 g/L, [sulfite] = 0.5 mM, [Cont] = 10.0 μM, pH 8.0, 92.9% in 30 min	$SO_4^{\bullet-}$	[40]
FeS	Grinding	Propranolol	[Cata] = 0.02 g/L, [sulfite] = 1.0 mM, [Cont] = 10.0 μM, pH 6.0, 95% in 20 min	$SO_4^{\bullet-}$ (main) and •OH	[131]
$Fe_xMo_{1\text{-}x}S_2$	One-pot hydrothermal method	Propranolol	[Cata] = 0.1 g/L, [sulfite] = 1.0 mM, [Cont] = 10.0 μM, pH 4.0, 90% in 30 min	$SO_5^{\bullet-}$ and $SO_4^{\bullet-}$	[43]
$CuFe_2O_4$	MOF-templated method and calcination	P-acetamidophenol, iohexol, benzoic acid	[Cata] = 0.1 g/L, [sulfite] = 0.5 mM, [Cont] = 10.0 μM, pH 8.0, over 80% in 30 min	$SO_4^{\bullet-}$ (main) and •OH	[42]
$CuFe_2O_4$	Commercial use	Metoprolol	[Cata] = 0.1 g/L, [sulfite] = 0.5 mM, [Cont] = 10.0 μM, pH 8.0, over 80% in 30 min	$SO_4^{\bullet-}$	[127]
$CoFe_2O_4$	Commercial use	Metoprolol	[Cata] = 0.5 g/L, [sulfite] = 2.0 mM, [Cont] = 10.0 μM, pH 10.0, 80.3% in 40 min	$SO_4^{\bullet-}$ and •OH	[34]
$NiFe_2O_4$	Commercial use	Estriol	[Cata] = 0.1 g/L, [sulfite] = 0.1 mM, [Cont] = 10.0 μM, pH 9.0, 87.6% in 60 min	$SO_5^{\bullet-}$ (main), $SO_3^{\bullet-}$ and •OH	[128]
$CoMn_{0.2}Fe_{1.8}O_4$	Sol-gel auto- combustion route	Orange II	[Cata] = 0.6 g/L, [sulfite] = 9.62 mM, [Cont] = 60 mg/L, pH 8–10, 85.4% in 120 min	Mn(III), $SO_4^{\bullet-}$ and •OH	[130]
Co embedded in N-doped carbon nanotubes	Thermal process	Methyl orange	[Cata] = 0.5 mM, [sulfite] = 5.0 mM, [Cont] = 20 mg/L, 96% in 20 min	$SO_4^{\bullet-}$ and •OH	[189]
$Cu(OH)_2$	Commercial use	N-acetyl-*para*-aminophenol	[Cata] = 0.01 mM, [sulfite] = 1.0 mM, [Cont] = 10.0 μM, pH 10.0, 80.3% in 40 min	$SO_5^{\bullet-}$ (main), $SO_4^{\bullet-}$ and •OH	[200]
Silica-supported copper	Complexation-adsorption-combustion method	As(III)	[Cata] = 0.1 g/L, [sulfite] = 0.1 mM, [Cont] = 5.0 μM, pH 8.0, ~90% in 60 min	$SO_5^{\bullet-}$, $SO_4^{\bullet-}$ (main) and •OH	[41]
Silica-supported cobalt	Complexation-calcination process	Orange II	[Cata] = 0.25 g/L, [sulfite] = 1.0 mM, [Cont] = 20.0 μM, pH 9.0, 79.4% in 20 min	surface-bound and free $SO_4^{\bullet-}$	[123]
Rectorite(containing 4.21% Fe)	Commercial use	Methyl orange	[Cata] = 2.0 g/L, [sulfite] = 5.0 mM, [Cont] = 20 mg/L, pH 3.5, 79.4% in 180 min	$SO_4^{\bullet-}$ (main) and •OH	[213]

[125] investigated the activation of sulfite using synthetic lithium cobalt oxide and found that oxygen vacancies in the catalyst drove sulfite activation to generate $SO_3^{\bullet-}$. Besides, the use of supports (e.g., silica) is also a feasible strategy to enhance the catalytic activity and stability of metal oxides [41,126].

$$\equiv Fe^{3+} + HSO_3^- + OH^- \rightarrow \equiv Fe^{2+} + SO_3^{\cdot-} + H_2O \tag{35}$$

$$2 \equiv Fe^{2+} + HSO_3^- + H_2O \rightarrow 2 \equiv Fe^{3+} + SO_4^{\cdot-} + OH^- \tag{36}$$

Spinel ferrites (MFe_2O_4, M = Zn, Co, Cu and Ni) are also employed for sulfite activation due to their low cost, easy preparation, excellent activity, magnetic property, high stability and reusability [34,127–129]. Among them, the formation of M−OH complexes on the catalyst surface is essential to enhance the catalytic activity. Compared to conventional hydrothermal and sol–gel combustion methods, $CuFe_2O_4$ derived from metal-organic frameworks-templated method has outstanding advantage in accelerating sulfite activation due to the increased active sites induced by large surface area and pore volume [42]. Additionally, doping Mn into $CuFe_2O_4$ can further improve the catalytic performance and doping level is a crucial factor [130].

2.2.3. *Metal sulfides*

Similar to metal oxides, metal sulfides have been investigated in activating sulfite [43,131]. Excitingly, the performance of FeS/sulfite system (95.0%) for propranolol degradation is much higher than that of FeS/peroxydisulfate (36.0%) and FeS/peroxymonosulfate (35.0%) systems, signifying that sulfite is a good substitute for persulfate to generate $SO_4^{\bullet-}$ [131]. However, although FeS/sulfite system can efficiently degrade propranolol, iron ions from FeS leaching actually accounts for sulfite activation, namely “homogenous activation”. In the future research, the difference in contaminant removal between sulfite activation and persulfate activation should be compared from multiple perspectives, including removal efficiency, chemical dosage, sulfite/persulfate decomposition and product toxicity, to thoroughly evaluate the feasibility of replacing persulfate with sulfite.

Inspired by sulfite oxidation catalyzed by sulfite oxidase enzyme, single Fe atoms confined in two-dimensional MoS_2 are constructed via one-pot hydrothermal method [43]. The catalysts with dual Fe-Mo active sites drive the efficient activation of sulfite and $SO_5^{\bullet-}$ are identified as the major contributor to propranolol degradation. Fan et al. [132] reported *in-situ* photoelectrochemical activation of sulfite with MoS_2 photoanode to produce oxysulfur radicals for the conversion of ammonia to nitrogen. Moreover, the conversion efficiency can be further improved by using MoS_2/WS_2 hybrid photoanode [133]. It is worth noting that sulfite also acts as a hole scavenger in the photoelectrocatalytic system.

2.3. *Photocatalytic activation of sulfite*

Recently, the photocatalytic activation of sulfite under visible light or simulated sunlight irradiation has received increasing attention in order to expand the utilization of solar energy. In this regard, photoelectrons and holes can be produced from photocatalysts under visible light irradiation, such as nitrogen vacancy doped carbon nitride [134], bismuth oxybromide [135,136] and bismuth vanadate [44,137]. The generated holes can activate sulfite to form $SO_3^{\bullet-}$ and the detailed mechanisms are expressed as Fig. 2. Meanwhile, due to its hole-scavenging capability, the introduction of sulfite can enhance the separation efficiency of photogenerated electron/hole pairs in photocatalysts, leading to the improved effectiveness in pollutant elimination [137–139]. Nevertheless, some different voices regarding the role of $SO_3^{\bullet-}$ appear [140]. Specifically, the generated $SO_3^{\bullet-}$ are unstable and can further react with dissolved oxygen to produce $SO_5^{\bullet-}$ and $SO_4^{\bullet-}$, and consequently $SO_4^{\bullet-}$, $O_2^{\bullet-}$ and •OH work together to degrade contaminants [141–143]. Besides, some metal-based photocatalysts including $Zn_xCu_{1-x}Fe_2O_4$ and Fe(III)-impregnated N-doped TiO_2 have a dual functionality in providing holes and acting as catalysts for sulfite activation, leading to the generation of dominant $SO_4^{\bullet-}$ [129,144]. Therefore, selecting a suitable catalyst is the key to the photocatalytic activation of sulfite, which is closely related to the reaction mechanism of the synergistic effects.

At present, a large number of sulfite-based AOPs have been constructed and investigated, mainly focusing on the activation of sulfite with metal-based catalysts. Heterogeneous catalysts can significantly reduce the leaching of metal ions but inevitable, thereby limiting their practical application in water treatment. Based on this, the activation of sulfite using non-metallic catalysts such as carbon nanotube, graphene and biochar is very appealing and worthy of research, which is expected to fundamentally solve the problem of metal leaching. In addition, few studies have evaluated the toxicity changes during the degradation using sulfite-based AOPs, despite degradation intermediates and pathways involved have been proposed. As known, degradation process is uncertain and may produce more toxic by-products, posing a threat to the environment. Accordingly, the toxicity assessment of organics degradation by sulfite-based AOPs needs to be concerned.

3. Overview of recent progresses in sulfite-based ARPs

In order to overcome the leaching of metal ions, radiation technology has also been explored for sulfite activation. Light sources for sulfite activation can be classified as UV light, visible light, UV–Vis light and simulated sunlight. Due to the complicated chemical properties of sulfite, each of light sources mentioned above leads to varied reaction mechanisms (Fig. 2). Especially, sulfite can be photolyzed by UV irradiation to produce reductive species, namely “ARPs” [45,56,145], which are basically different from sulfite-based AOPs in Section 2. Collectively,

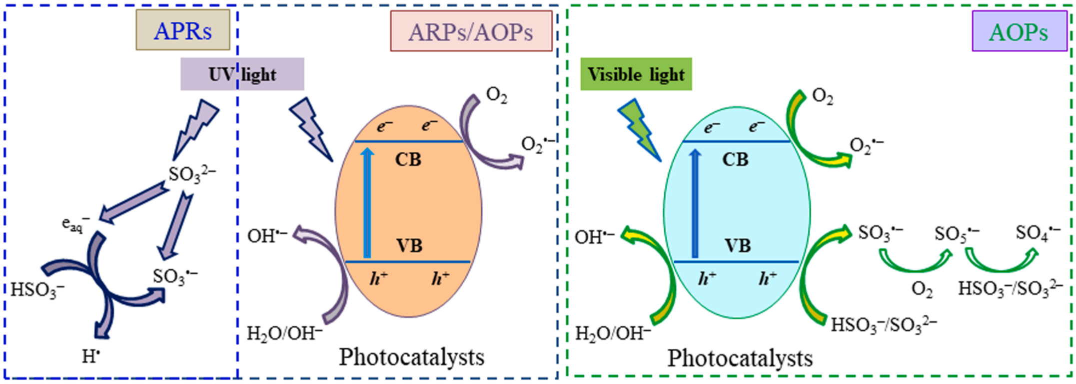

Fig. 2. The mechanism for the photocatalytic activation of sulfite.

ARPs decompose contaminants directly via *in-situ* generated reductive species, which can be converted into simple and biodegradable intermediates instead of transferring them to another phase or producing more toxic intermediates [146].

3.1. Characteristic and mechanism of reductive species generated during UV/sulfite process

Although sulfite shows a certain efficacy in directly removing halogenated disinfection by-products, improvement performance is still needed [147,148]. As reported, sulfite has a strong UV absorption capacity [149] and its maximum absorption wavelength locates at 275 nm [52,150]. Consequently, sulfite can be photoionized under UV irradiation to generate •H, $SO_3^{\bullet -}$ and e_{aq}^- (Eqs. (37), 38) [146], and its ionization efficiency is much better than other sulfur-containing reducing agents (e.g., sulphide and dithionite) [151]. Moreover, the quantum yields of e_{aq}^- in UV/sulfite process are as high as 0.108–0.391 [152]. It is argued that the shorter the UV wavelength, the higher the energy, and thus exciting molecules stronger. Consequently, water can be photolyzed directly by UV_{185} (main UV wavelength locates 185 nm) to generate •H, •OH and e_{aq}^- (Eqs. (39, 40)) [153], while this unique phenomenon cannot be observed at UV_{254} [154]. In recent years, UV/sulfite process has been regarded as a novel ARPs for the elimination of contaminants from water [155–159].

$$SO_3^{2-} + hv \rightarrow SO_3^{\bullet -} + e_{aq}^- \tag{37}$$

$$HSO_3^- + hv \rightarrow SO_3^{\bullet -} + \bullet H(k = 2.0 \times 10^7 M^{-1}s^{-1}) \tag{38}$$

$$H_2O + hv_{185} \rightarrow H^+ + \bullet OH + e_{aq}^-, \phi(+e_{aq}^-) = 0.045 \tag{39}$$

$$H_2O + hv_{185} \rightarrow \bullet H + \bullet OH, \phi(+\bullet OH) = 0.33 \tag{40}$$

Among the reductive species generated from UV/sulfite process, e_{aq}^- have the strongest reducing ability (standard redox potential, −2.9 V). Due to the unique chemical structure of e_{aq}^- (a cavity structure formed by bare electrons surrounding water molecules), its diffusion coefficient and mobility in aqueous solution is relatively high, which is favorable for removing contaminants [160]. In general, e_{aq}^- have the following characteristics: (1) acting as a nucleophile to attack organics with a low electron cloud density; (2) exhibiting high reactivity toward organics with electron-withdrawing groups; (3) dehalogenating when it reacts with halogenated organics (Eq. (41)) [161]. As a conjugate acid of e_{aq}^-, •H are often present in the aqueous solution along with e_{aq}^-. The standard redox potential of •H is −2.3 V, so it has a strong reducing ability, especially for inorganic compounds [162,163]. Taking monochloroacetic acid as an example, e_{aq}^- and •H can lead to totally different reductive degradation pathways (Eqs. (42, 43)) [149]. Therefore, monochloroacetic acid has been well established as a probe compound to identify the generation and contribution of e_{aq}^-. When solution pH is 3.0, •H dominate in the system via transformation of e_{aq}^- at excessive H^+ (Eq. (44)) [51]. Meanwhile, •H can undergo H-abstraction reactions with saturated molecules or addition reactions with unsaturated molecules (Eqs. (45, 46)) [164]. Besides, $SO_3^{\bullet -}$ can also be produced with a redox potential of 0.63 V, thereby showing both oxidation and reduction capabilities [164]. When dissolved oxygen and other scavengers (e.g., inorganic ions and dissolved organic matters) are absent, $SO_3^{\bullet -}$ can react with e_{aq}^- to regenerate sulfite or recombine to form sulfate (Eqs. (47, 48)) [51,52]. Moreover, $SO_3^{\bullet -}$ have the highest reactivity under strongly alkaline conditions (pH > 12.0).

$$e_{aq}^- + RX \rightarrow RX^- \rightarrow \bullet R + X^- \tag{41}$$

$$\bullet H + ClCH_2CO_2H \rightarrow \bullet CHClCO_2H + H_2 \tag{42}$$

$$e_{aq}^- + ClCH_2CO_2H \rightarrow \bullet CHCO_2H + Cl^- \tag{43}$$

$$e_{aq}^- + H^+ \rightarrow \bullet H(k = 2.3 \times 10^{10} M^{-1}s^{-1}) \tag{44}$$

$$\bullet H + CH_3OH \rightarrow \bullet CH_2OH + H_2 \tag{45}$$

$$\bullet H + CH_2 = CH_2 \rightarrow \bullet CH_2CH_3 \tag{46}$$

$$SO_3^{\bullet -} + e_{aq}^- \rightarrow SO_3^{2-} \tag{47}$$

$$SO_3^{\bullet -} + SO_3^{\bullet -} + H_2O \rightarrow SO_4^{2-} + SO_3^{2-} + 2H^+ \tag{48}$$

However, some organic pollutants are difficult to degrade by UV/sulfite process. For example, when UV/sulfite process encounters urea from swimming pool, it exhibits extremely poor performance, much lower than UV/peroxydisulfite and UV/H_2O_2 processes [165], which can be interpreted as the low reactivity of e_{aq}^-/•H and urea ($k_1(\bullet H) < 3.0 \times 10^4$ $M^{-1}s^{-1}$, $k_2(e_{aq}^-) = 3.0 \times 10^5$ $M^{-1}s^{-1}$) [166,167].

Currently, conventional low-pressure mercury lamps are used as the major UV source to drive sulfite-based ARPs [47,149,168]. Nevertheless, several application challenges are faced, such as low energy efficiency and high cost. As an alternative UV source, UV-light emitting diodes (UV-LEDs) have become a research hotspot, mainly because they have the merits of environmental friendliness, low cost, less energy consumption and long lifetime [169]. To date, less information is known about the effectiveness and mechanisms of the UV-LEDs/sulfite ARPs on the degradation of organic pollutants. The only existing research involving the activation of sulfite with UV-LEDs is the reduction of graphene oxide by e_{aq}^- [170].

The reaction mechanisms for UV/sulfite process have been widely explored. For example, e_{aq}^- are identified as the dominated species under alkaline conditions for contaminants elimination [49,50]. Jung et al. [171] found that the removal mechanism of bromate in the UV/sulfite process showed a remarkable dependence on sulfite concentration. Specifically, direct photolysis dominates at low concentrations, while e_{aq}^-/•H can play a leading role at high concentrations. Xie et al. [172] reported that both direct photolysis and e_{aq}^- contributed to the debromination of 4-bromophenol. The introduction of sulfite also transforms the degradation pathway of atrazine under UV irradiation, from direct hydroxylated dechlorination to indirect e_{aq}^-/•H-mediated reduction [173]. Among, UV photolysis and e_{aq}^- mainly contribute dechlorination, while •H are crucial for the hydrogenation and ring cleavage of atrazine. In addition, Xiao et al. [174,175] explored the removal of bromate by UV/sulfite process in lab and pilot studies. They showed that e_{aq}^-, •H and both of them were main reactive species responsible for bromate removal under alkaline conditions (pH > 9.0), acidic conditions (pH 4.0) and neutral conditions (pH 7.0), respectively. Similar conclusion is also obtained during the degradation of diclofenac by UV/sulfite process [145]. It can be seen from the above studies that the reaction mechanism in the UV/sulfite process includes direct UV photolysis and indirect sulfite photolysis (ie, the production of reductive species), and their contribution is mainly determined by the relative adsorption of contaminants and sulfite under UV irradiation. In particular, UV photolysis can easily decompose some organic contaminants (e.g., 2, 4, 6-trichlorophenol) and plays a leading role even in the presence of sulfite. At the same time, environmental conditions such as solution pH, sulfite concentration, dissolved oxygen concentration, UV intensity and wavelength will also affect the reaction mechanism.

3.2. Enhanced strategies for UV/sulfite process

In general, e_{aq}^- generated by photoionization of sulfite require a large amount of sulfite and high pH due to the protonation of sulfite and the scavenging effects of coexisting species (such as H^+, HSO_3^-, dissolved oxygen) [176]. To improve the yield and availability of e_{aq}^- in UV/sulfite process, some efforts have been made. For example, UV lamp with a high photon flux is employed to promote e_{aq}^- yield [35,161]. The addition of iodide into UV/sulfite process can greatly enhance contaminant removal

[46,55]. This can be explained by the fact that both sulfite and iodide act as e_{aq}^- precursors and sulfite can reduce the e_{aq}^- scavenging by reactive iodine species. Bismuth oxyiodide is also used as a sustainable source of I^-, thereby accelerating e_{aq}^- yield [56]. Besides, it is meaningful to investigate the effect of UV light at different wavelengths on sulfite activation, possibly leading to different behaviors of organics degradation.

UV/sulfite process can also be served as a pretreatment to integrate other techniques for the synergistic removal of contaminants, including biological process, Fe(III) coagulation and electrochemical deposition [50,177,178]. For example, during the UV/sulfite-coupled electrochemical deposition system, the e_{aq}^- produced from UV/sulfite process can reduce Sb(V) to Sb(III) and then further reduce it to metal Sb by cathodic reduction, thus achieving Sb recovery [178].

The introduction of semiconductor photocatalysts (e.g., ZnO and TiO_2) into UV/sulfite process is an effective method to simultaneously produce oxidative and reductive species (Fig. 2) (Eqs. (37, 38, 49–52)) [179,180]. Such technique can achieve the complete degradation of halogenated organic compounds as much as possible.

$$semiconductor + hv \rightarrow h_{VB}^+ + e_{CB}^- \tag{49}$$

$$h_{VB}^+ + H_2O \rightarrow \bullet OH + H^+ \tag{50}$$

$$h_{VB}^+ + OH^- \rightarrow \bullet OH \tag{51}$$

$$e_{CB}^- + O_2 \rightarrow O_2^{\bullet -} \tag{52}$$

4. Key factors affecting the removal performance in sulfite-based AOPs/ARPs

As discussed above, sulfite can be activated to produce highly reactive species and the types of reactive species generated are highly dependent on activation methods. According to the redox characteristics of reactive species, activated sulfite systems can be classified into AOPs, ARPs and AOPs/ARPs. In previously reported literatures, these processes are mostly used in the removal of contaminants, such as phenolic compounds [73,108], dyes [27,39,135], perfluoroalkyl substances [35,45,53], pesticides/herbicides [94,129], bromate [156,175], pharmaceutical and personal care products [36,80,81]. It should be emphasized that sulfite-based ARPs can not only effectively decompose halogenated organic compounds, but also can achieve dehalogenation releasing halogen ions, thereby greatly reducing their toxicity, especially for perfluoroalkyl substances. In addition, activated systems are also applied in metals detoxification [48–50,74,108] and bacterial inactivation [95]. In these processes, some key factors affecting the removal performance including dissolved oxygen, sulfite dosage, pH and water matrix are discussed as follows.

4.1. Dissolved oxygen

Dissolved oxygen is ubiquitous in aquatic environment, which plays an important role in sulfite activation. Especially, dissolved oxygen is engaged in the formation of metal-sulfite complexes and subsequent oxysulfur radicals, markedly affecting the removal performance. For example, the degradation efficiency of aniline is greatly decreased from 70.0% to 10.0% without dissolved oxygen, which is limited by the cycle of Fe(II)/Fe(III) and the conversion of $SO_3^{\bullet -}$ to $SO_5^{\bullet -}$ [67]. Similarly, Wang et al. [62] showed that the degradation of diclofenac could be completely inhibited under purging nitrogen. Chen et al. [68] proposed an aeration-assisted Fe(II)/sulfite process for chloramphenicol degradation. They found that the pseudo first-order rate constant increased from 6.0×10^{-4} to 1.38×10^{-2} min^{-1} as the concentration of dissolved oxygen increased within the range of 0–6.0 mg/L, and then remained almost unchanged as further increasing its concentration, which was due to the rate-determining step of $SO_3^{\bullet -}$ formation and the principle of oxygen compensation. In addition, during sulfite activation, dissolved oxygen in water is rapidly consumed in the initial stage and then gradually returns to the initial level [74,128], which also confirms its key role. Interestingly, the absence of dissolved oxygen can completely inhibit the degradation of 4-chlorophenol in Cr(VI)/sulfite system, but almost does not affect the reduction of Cr(VI) [111].

Chen et al. [131] investigated the effect of the generation method of dissolved oxygen on FeS/sulfite process and found that the degradation of propranolol under purging oxygen was inhibited compared to mechanical stirring. The authors explained as three aspects. 1) Dissolved oxygen under mechanical stirring was sufficient to achieve sulfite activation. 2) The structural Fe(II) in FeS would be converted to Fe(III) under aerobic conditions, thus changing the dissolution. 3) Large bubbles generated by purge might delay the transport of electrons between reactive species.

Qiao et al. [181] examined the kinetics and mechanisms of bromate removal by sulfite in the absence and presence of oxygen. The results showed that the presence of oxygen would lead to the over-stoichiometric sulfite consumption ($-\Delta[sulfite]/\Delta[bromate]$ were 3.33 and 15.63 without and with oxygen, respectively). The authors proposed that $SO_3^{\bullet -}$ were produced through reducing bromate by H_2SO_3 and were responsible for bromate removal under anaerobic conditions, while the generated $SO_3^{\bullet -}$ under aerobic conditions would react with oxygen and eventually be converted into dominant $SO_4^{\bullet -}$.

In addition, dissolved oxygen is of great concern in sulfite-based ARPs due to its scavenging effect, as described in Eqs. (53, 54). For example, the removal efficiency of bromate in UV/sulfite process after reaction (20) min decreases from 95% to 82% when dissolved oxygen is absent [175]. Significant inhibitory effect also occurs in the degradation of 4-bromophenol [172]. Excitingly, the scavenging effect of dissolved oxygen toward e_{aq}^- can be minimized up to certain extent by the chain reactions involving $SO_3^{\bullet -}$ oxidation (Eqs. (3–7)). Besides, Xie et al. [49] found that dissolved oxygen (about 8.0 mg/L) exhibited a negligible effect on Cr(VI) reduction by UV/sulfite process, which might be due to the consumption of dissolved oxygen by excess sulfite (5.0 mM). Similar result is reported in the degradation of per- and polyfluoroalkyl substances by high photon flux UV/sulfite process [35,161]. Under the circumstances, more than 94.0% of perfluorooctane sulfonate can be decomposed even if 5.0 mg/L of dissolved oxygen is presented. Very recently, some studies reported that the presence of dissolved oxygen in UV/sulfite process could transform the reaction pathway from e_{aq}^- reduction to oxysulfur radicals oxidation [182–184].

In general, the role of dissolved oxygen on sulfite-based AOPs/ARPs is unclear and warrants further investigation. Due to its high reaction rate with reactive species ($SO_3^{\bullet -}$ and e_{aq}^-) generated from sulfite-based AOPs/ARPs, it not only affects the degradation behavior of contaminants, but also changes the reaction mechanisms. Especially, contradictory results can also occur in the same constructed system, many of which may be due to the fact that the degradation experiments is not strictly controlled under anaerobic conditions, and the concentration of dissolved oxygen is not quantitatively identified and monitored. Therefore, more research should be conducted to explore the degradation performance and mechanisms of contaminants by sulfite-based AOPs/ARPs in the presence and absence of oxygen.

$$e_{aq}^- + O_2 \rightarrow O_2^{\bullet -} (k = 1.9 \times 10^{10} M^{-1} s^{-1}) \tag{53}$$

$$\bullet H + O_2 \rightarrow HO_2^{\bullet} \leftrightarrow H^+ + O_2^{\bullet -} (k = 1.2 \times 10^{10} M^{-1} s^{-1}) \tag{54}$$

4.2. Sulfite concentration

The concentration of sulfite is crucial to the oxidative/reductive degradation of contaminants during sulfite activation, which is closely related to the amounts and types of reactive species generated. In most sulfite-based AOPs, sulfite concentration shows a volcanic pattern in removing contaminants. For example, Chen et al. [131] reported that the degradation rate of propranolol in the FeS/sulfite system increased from 0.009 to 0.184 min^{-1} as increasing sulfite concentration from 0.1 to 1.0 mM, and then decreased to 0.106 min^{-1} as it further increased to 2.0 mM because of the depletion of SO$_4^{\bullet-}$ by excess sulfite. In sulfite-based ARPs, the degradation rate of contaminants is linearly related to sulfite concentration within an appropriate range, and the molar ratio of sulfite to contaminants is as high as 530 [27,47,185]. However, Yu et al. [145] presented that the degradation rate of diclofenac decreased from 0.1541 to 0.1449 min^{-1} when sulfite concentration further increased from 8 to 32 mM. As a result, the use of excess sulfite should be avoided.

4.3. pH

Solution pH is considered to be a key parameter in sulfite activation, which can affects the interaction between the catalysts, sulfite and target pollutants as well as the yield of reactive species, thereby affecting the degradation efficiency of contaminants. As shown in Fig. 3a, b, the distribution of sulfite species is pH-dependent. Since the pK$_a$ of sulfite is 7.2, HSO$_3^-$ dominates when the pH is 4.0–7.0 and SO$_3^{2-}$ dominates when the pH is greater than 9.0.

In UV/sulfite-based ARPs, the optimum pH for contaminant removal is about 8–10, and further increasing pH only slightly affects the degradation rate [168,186]. On one hand, the significant increase in degradation rate with pH is highly related to the fraction of SO$_3^{2-}$. As reported, SO$_3^{2-}$ has a higher molar absorption coefficient and quantum yield than HSO$_3^-$ under UV irradiation [65,149], and thus can be easily photolyzed to produce high reduction potential of e$_{aq}^-$ under alkaline conditions. On the other hand, the protonation of SO$_3^{2-}$ can occur at low pH, so the amount of e$_{aq}^-$ will be decreased due to the scavenging effects of H$^+$ and HSO$_3^-$ [175]. Differently, Yu et al. [145] reported that the degradation rate of diclofenac decreased with increasing pH within pH range of 6.0–10.0. In addition, pH can play an important role in interconversion between •H and e$_{aq}^-$. For example, Xiao et al. [175] reported the reductive species that responded to bromate removal in the UV/sulfite process were •H at pH 4.0, e$_{aq}^-$ at pH greater than 9.0 and their coexistence at pH 7.0.

By comparison, the role of pH is complicated in sulfite-based AOPs. Firstly, pH can affect the species distribution of metal ions in homogenous metal/sulfite process (Fig. 3c, d). For example, the effective working pH for Fe(III)/Fe(II) or Mn(II) is lower than 4.0 [27], while that for Cu(II) or Co(II) is under alkaline conditions [91,95]. For heterogeneous catalysts, pH also has an effect on its surface charge, thus affecting the interaction with sulfite [34,42,128,144]. The surface charge of catalyst is negative when the solution pH value is over the pH at zero point of charge, which leads to the generation of electrostatic repulsion between the negatively charged surface of catalysts and sulfite, thereby causing the decline of degradation efficiency. Secondly, solution pH influences the speciation of contaminants and its deprotonation generally is conducive to the electrophilic attack of reactive species [128]. As last, pH can also adjust the generation and transformation of reactive species in activated sulfite process. For instance, alkaline pH can accelerate the transformation of SO$_5^{\bullet-}$ to SO$_4^{\bullet-}$ [34] and SO$_4^{\bullet-}$ to •OH (Eq. (55)) [124]. Hence, an appropriate pH for contaminant removal should be selected based on the activated sulfite process.

$$SO_4^{\cdot-} + OH^- \rightarrow SO_4^{2-} + \cdot OH (pH > 8) \tag{55}$$

4.4. Water constituents

Inorganic anions (e.g., chloride, bicarbonate, phosphate, nitrate and nitrite) and natural organic matters are common constituents in actual water. Their effects have been widely examined to assess the application potential of sulfite-based AOPs/ARPs. As reported in most literatures [40,78,131,187,188], the presence of chloride, bicarbonate or phosphate exhibited inhibitory effects on contaminants removal because they can react with SO$_4^{\bullet-}$/•OH to produce less reactive radicals. For example, the degradation efficiency of iohexol in CuFe$_2$O$_4$/sulfite system is reduced by about 50% at 2.0 mM chloride ions, due to the formation of chlorine radicals via the reaction of SO$_4^{\bullet-}$ with chloride ions [42]. Chen et al. [68] investigated the effect of halogen ions on

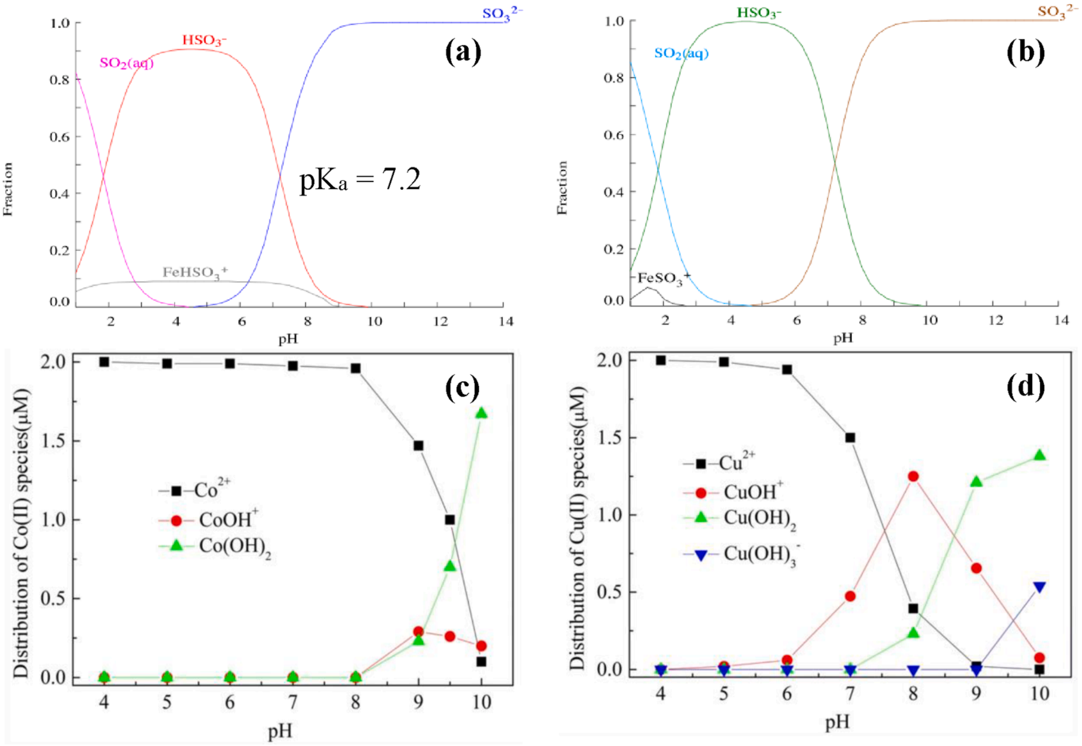

Fig. 3. Species distributions of sulfite in Fe(II)/sulfite (a) and Fe(III)/sulfite (b) systems [27], and species distributions of metal ions in Co(II)/sulfite (c) and Cu(II)/sulfite (d) systems [91].

chloramphenicol degradation in Fe(II)/sulfite system. The result showed that the inhibitory effect followed iodide > bromide > chloride, which corresponded to their reactivity with $SO_4^{\bullet-}$. In addition, the presence of phosphate and bicarbonate makes the catalyst surface complex, retarding the interaction between catalytic sites and sulfite [126]. Differently, Wu et al. [189] reported that the addition of bicarbonate could significantly accelerate the degradation of methyl orange. The authors revealed that bicarbonate could complex with structural Co(II) in catalysts and thus promote the oxidation of Co(II) to Co(III), resulting in the formation of high-valent cobalt species.

Compared with nitrate, nitrite has a more significant inhibition on chloramphenicol degradation, and the degradation rate decreases from 9.4×10^{-3} to 9.2×10^{-3} and 5.2×10^{-3} min^{-1} in the presence of nitrate and nitrite, respectively [68]. It should be highlighted that nitrate/nitrite are not only common water components affecting the removal performance, but also are widely used as scavengers for e_{aq}^- and •H because of their distinct second-rate constants (Eqs. (56–59)) [164].

$$e_{aq}^- + NO_2^- \rightarrow (NO_2^{\cdot})^{2-} (k = 4.1 \times 10^9 M^{-1} s^{-1}) \tag{56}$$

$$e_{aq}^- + NO_3^- \rightarrow (NO_3^{\cdot})^{2-} (k = 9.7 \times 10^9 M^{-1} s^{-1}) \tag{57}$$

$$\cdot H + NO_2^- \rightarrow NO^{\cdot} + OH^- (k = 7.1 \times 10^8 M^{-1} s^{-1}) \tag{58}$$

$$\cdot H + NO_3^- \rightarrow (NO3H^{\cdot})^- \left(k = 1.4 \times 10^6 M^{-1} s^{-1}\right) \tag{59}$$

Humic acid is a main constituent of natural organic matters and its reaction rates with •OH and $SO_4^{\bullet-}$ are 1.4×10^4 and 6.8×10^3 L mgC^{-1} s^{-1}, respectively, so it can compete with target pollutants for $SO_4^{\bullet-}$/•OH oxidation [190,191]. Xiao et al. [174] indicated that high concentrations of humic acid significantly inhibited the removal of bromate during UV/sulfite process in a pilot study. Likewise, humic acid can interface with the photolysis of sulfite, which leads to the decrease in the yield of reductive species [157]. Jung et al. [192] reported that the removal of bromate was promoted by humic acid at low concentrations, but that was inhibited at concentrations higher than 5.0 mg/L. In addition to its scavenging effect, humic acid can also act as a complexing agent to complex with metal ions or heterogeneous metal catalysts, thus indirectly affecting the removal performance of contaminants [42,131].

5. Identification of reactive species and determination methods

In section 2 and 3, we have summarized the activation methods of sulfite and the reactive species (including $SO_3^{\bullet-}$, $SO_4^{\bullet-}$, $SO_5^{\bullet-}$, •OH, high-valent metals, e_{aq}^- and •H) involved are highly dependent on activation methods. Identifying reactive species are essential because it helps to explore the degradation behavior, mechanisms and pathways of contaminants in-depth. Till now, the main technologies for detection of reactive species in sulfite-based AOPs/APRs include quenching studies, chemical probe methods, and electron spin resonance techniques.

5.1. Quenching studies and chemical probe method

Quenching studies refers to the use of specific chemical probes/reagents to directionally eliminate the reactive species generated in the system, so as to distinguish the relative contributions of each reactive species according to the inhibition degrees of target pollutants. Table 5 lists the reaction second-order rate constants between the selected probe compounds/quenchers and the corresponding reactive species.

Alcohols are generally regarded as scavengers to identify the relative contributions of $SO_4^{\bullet-}$ and •OH [24,193–195]. Specifically, alcohols containing α-hydrogen (e.g., ethanol and methanol) can effectively quench both $SO_4^{\bullet-}$ and •OH, while alcohols without α-hydrogen (e.g., *tert*-butanol) only capture •OH due to distinct second-order rate constants [196]. In contrast, the reactivity of other oxysulfur radicals including $SO_3^{\bullet-}$ and $SO_5^{\bullet-}$ is low toward alcohols ($<10^3$ M^{-1} s^{-1}) [196,197]. In addition, atrazine, nitrobenzene and benzoic acid are also used as chemical probes or scavengers for $SO_4^{\bullet-}$ and •OH (for atrazine, $k_1(SO_4^{\bullet-}) = 4.2 \times 10^9$ M^{-1} s^{-1}, $k_2(\bullet OH) = 2.4–3.0 \times 10^9$ M^{-1} s^{-1}; for benzoic acid, $k_3(SO_4^{\bullet-}) = 1.2 \times 10^9$ M^{-1} s^{-1}, $k_4(\bullet OH) = 4.2 \times 10^9$ M^{-1} s^{-1}; for nitrobenzene, $k_5(SO_4^{\bullet-}) = 8.4 \times 10^5$ M^{-1} s^{-1}, $k_6(\bullet OH) = 3.9 \times 10^9$ M^{-1} s^{-1}) [24,190,196]. Moreover, $SO_4^{\bullet-}$ and •OH can be quantified by chemical competition kinetic experiments with radical scavengers. Of note, the concentration of selected quenching agents is critical due to the involvement of multi-reactive species during sulfite activation. Tert-butanol at excess dosage can also quench $SO_4^{\bullet-}$, besides •OH. For example, Dong et al. [60] firstly selected 250 mM methanol to completely quench $SO_4^{\bullet-}$ and •OH, obtaining the total contributions of 89.04%, and then 10 mM *tert*-butanol was selected to discern the relative contributions of $SO_4^{\bullet-}$ and •OH, accounting for 23.29% and 65.75%, respectively. However, some studies stated that hydrophilic alcohols (e.g., methanol and *tert*-butanol) were difficult to approach the surface of heterogeneous catalysts, making it difficult to quench surface-bound radicals [13,24,126].

For $SO_3^{\bullet-}$, its role must be determined in an oxygen-free conditions due to its high reactivity with oxygen (1.0–2.5 × 10^9 M^{-1} s^{-1}) [44,64,196]. Besides, $SO_3^{\bullet-}$ has a high reaction rate with crocin (1.0 × 10^9 M^{-1} s^{-1}) [198], which has been used as a chemical probe to measure the yield of $SO_3^{\bullet-}$ [134].

As for $SO_5^{\bullet-}$, Yuan et al. [67] determined the second-order rate constants between $SO_5^{\bullet-}$ and aniline, about $5.8 \pm 0.6 \times 10^6$ M^{-1} s^{-1}. Subsequently, they employed diphenylamine and ethanol as scavengers to ascertain the relative contributions of $SO_4^{\bullet-}$ and $SO_5^{\bullet-}$ on the degradation of aniline in the Fe(III)/sulfite system. Based on its reactivity, aniline is also used as an effective scavenger for $SO_5^{\bullet-}$ [43,199,200]. For example, the addition of aniline can markedly inhibit the degradation of propranolol and the degradation efficiency is decreased from 90.0% to 10.8% at 10 mM aniline, indicating that $SO_5^{\bullet-}$ are the main oxidants causing degradation in the $Fe_{0.36}Mo_{0.64}S_2$/sulfite system [43].

In addition to the above-mentioned radicals, high-valent metal species are also identified in sulfite-based AOPs, such as Fe(V)/Fe(IV) [80,87,89], Mn(III) [97] and Cr(V) [109]. Furthermore, their

Table 5
Second-order rate constants of the selected probe compounds/quenchers with different reactive species.

Quenching agents	Second-order rate constants (M^{-1} s^{-1})						Ref.
	$SO_3^{\bullet-}$	$SO_4^{\bullet-}$	$SO_5^{\bullet-}$	•OH	e_{aq}^-	•H	
Methanol	/	0.9–1.3 × 10^7	/	0.8–1.0 × 10^9	/	/	[164,214]
Ethanol	< 2.0 × 10^3	1.6 × 10^7	< 1.0 × 10^3	1.9 × 10^9	/	/	[197]
Tert-butanol	< 1.0 × 10^3	4.0–9.1 × 10^5	< 1.0 × 10^3	3.8–7.6 × 10^8	/	/	[197,214]
Aniline	< 1.0 × 10^6	7.7 ± 0.5 × 10^9	5.8 ± 0.6 × 10^6	1.7 × 10^{10}	/	/	[67]
Diphenylamine	< 1.0 × 10^7	/	5.0 × 10^7	/	/	/	[199]
Crocin	1.0 × 10^9	/	/	/	/	/	[198]
Nitrate	/	/	0.05–2.1 × 10^6	/	9.7 × 10^9	1.4 × 10^6	[164,215]
Nitrite	/	9.8 × 10^8	/	1.0 × 10^{10}	4.1 × 10^9	7.1 × 10^8	[164,196]
Nitrous oxide	/	/	/	/	9.1 × 10^9	2.1 × 10^6	[166]

/: No reported or used as the related chemical probes/quenchers.

contributions can be confirmed through the inhibitory effects of sulfoxides and the degradation products of sulfoxides [87,201]. As reported, Fe(V)/Fe(IV) can oxidize sulfoxides (e.g., dimethyl sulfoxide and methyl phenyl sulfoxide) into sulfones (e.g., dimethyl sulfone and methyl phenyl sulfone) via oxygen-atom transfer mechanism, respectively, which is essentially different the reaction of free radicals and sulfoxides, thereby discriminating their roles and contributions (Eqs. (60, 61)) [202–204].

$$Fe(IV) = O + (CH_3)_2SO \rightarrow (CH_3)_2SO_2 \tag{60}$$

$$2 \bullet OH + 2(CH_3)_2SO + O_2 \rightarrow 2(CH_3)_2SO_2H + HCHO + CH_3OH \tag{61}$$

Originating from the photolysis of sulfite, reductive species are produced, including $SO_3^{\bullet-}$, e_{aq}^- and •H. It was reported that nitrite was capable of quenching both e_{aq}^- and •H, but nitrate could only scavenger e_{aq}^- [153,164], leading to a clear role of e_{aq}^- and •H. Moreover, considering that saturated nitrous oxide in the solution will double the yield of $SO_3^{\bullet-}$ and react rapidly with e_{aq}^- [149], it can be employed to distinguish the contributions of $SO_3^{\bullet-}$ and e_{aq}^- [49,172]. In addition, the steady-state concentration of e_{aq}^- can be estimated using monochloroacetic acid as a chemical probe [149,176]. Likewise, nitrobenzene is also used to determine the steady-state concentration of e_{aq}^-, because it exhibits high reactivity towards e_{aq}^- (3.7×10^{10} M^{-1} s^{-1}) [170].

5.2. *Electron spin resonance spectroscopy*

Electron spin or paramagnetic resonance spectroscopy is a powerful and sensitive technique for detecting free radicals generated in chemical or biological processes [205,206]. Due to their short lifetime (e.g., 30–40 μs for $SO_4^{\bullet-}$ and 20 ns for •OH), spin-trapping agents are required to capture free radicals to form stable and clear spin adducts. The common used radical-trapping agent is 5,5-Dimethyl-1-pyrroline N-oxide (DMPO). As reported, the signals of DMPO-$SO_4^{\bullet-}$ adducts (aN = 13.7 G, aH = 10.0 G, aH = 1.41 G and aH = 0.78 G) and DMPO-•OH adducts (aN = 14.9 G and aH = 15.0 G) are observed through their typical hyperfine splitting constants (Fig. 4a, c), which are derived from the nucleophilic addition reaction of $SO_4^{\bullet-}$/•OH with DMPO [24,133]. Moreover, the evolution of $SO_4^{\bullet-}$/•OH with reaction times can also be obtained according to the ESR peak intensity (Fig. 4b) [24]. Of note, the reaction second-order rate constants between DMPO and $SO_4^{\bullet-}$ is low and the generated DMPO-$SO_4^{\bullet-}$ adducts are unstable, which makes it difficult to perform quantitative analysis [14]. Meanwhile, DMPO-$SO_4^{\bullet-}$ adducts can be converted into DMPO-•OH adducts at a considerably reaction rate through reacting with H_2O/OH^-, namely nucleophilic substitution reaction. Except for DMPO, 5-*tert*-Butoxycarbonyl-5-methyl-1-pyrroline-N-oxide is also utilized as a spin trapping agent for $SO_4^{\bullet-}$ and •OH. In addition, the signal of DMPO-$SO_3^{\bullet-}$ adducts (aH = 15.9 G and aN = 14.7 G) is identified and their signal intensities increase as the reaction proceeded (Fig. 4d) [137]. On the contrary, DMPO cannot trap $SO_5^{\bullet-}$ to produce the corresponding adduct signals even if $SO_5^{\bullet-}$ exists in the system [197].

As present, due to the diversity of the types and amounts of the reactive species generated from sulfite activation, the detection technologies of existing studies are difficult to precisely determining the contributions of reactive species. In the future research, more advanced technologies for identifying reactive species in a quantitative and qualitative way should be developed to gain an in-depth understanding about their respective contributions and reaction mechanisms.

6. Concluding remarks and future perspectives

In summary, this review presents the state-of-the-art development of

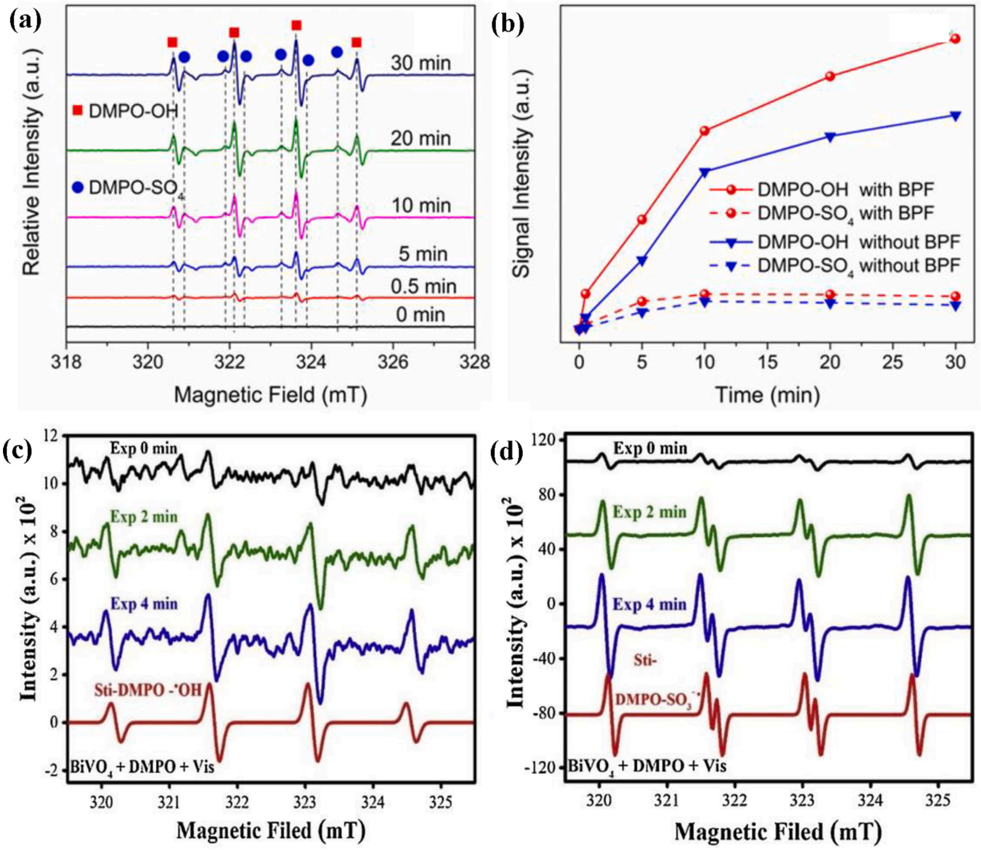

Fig. 4. ESR spectra of DMPO-•OH and DMPO-$SO_4^{\bullet-}$ adducts (a) and their intensity variations as a function of time (b) [24], and ESR spectra of DMPO-•OH (c) and DMPO-$SO_3^{\bullet-}$ (d) adducts in $BiVO_4$/sulfite/vis system [137].

sulfite-based AOPs/APRs to eliminate contaminants from water, with particular emphasis on the generation mechanisms and identification technologies of reactive species (including oxidative and reductive species) under different activation strategies, and key factors influencing the removal performance. Despite current researches have suggested the potential application of sulfite-based AOPs/ARPs in water treatment, further investigations are still required. Moreover, most researches still stay in laboratory exploration and are carried out in ultrapure water, so there is still a long way to go before practical application. Based on our review, several key points are proposed as follow:

(1) The concentration of sulfate ions generated during sulfite activation should be concerned, especially at photo/sulfite process. For example, the dosages of sulfite used in some studies are as high as 5–20 mM [44,49,168,207], which leads to the concentration of the generated sulfate higher than the Standards for Drinking Water Quality of China (250 mg/L, ~2.61 mM).

(2) The productivity of e_{aq}^- in the UV/sulfite process needs to be improved. Since e_{aq}^- have high reactivity with coexisting scavenger species (e.g., H^+, H_2O, dissolved oxygen and nitrate/nitrite), the amount of e_{aq}^- that can be used to degrade target pollutants is significantly reduced.

(3) In homogenous systems, how to accelerate the redox cycle of metal ions and the decomposition of metal-sulfito complexes is essential to increase the yield of $SO_4^{\bullet -}$ in the overall reaction. Moreover, the generation of metal sludge will increase the cost of secondary treatment, so how to reduce the dosage of metal ions or avoid the production of metal sludge are worthy of investigation.

(4) The development of environment-benign, cost-effective and high-performance heterogeneous catalysts with rational design has never stopped. Although heterogeneous metal catalysts can reduce the leaching of toxic metal ions to a certain extent and increase its reusability, metal leaching is still inevitable. Inspired by the effective activation of persulfate by metal-free carbocatalysts [208–211], the feasibility of activating sulfite with carbocatalysts (containing adjustable structures, abundant functional groups, structural defects and other catalytic sites) should be explored, which is expected to fundamentally solve the problem of metal leaching.

(5) The mechanisms of sulfite activation by various approaches are still unclear and warrant further investigation. In particular, the reactive species involved and their respective contributions vary with reaction conditions (e.g., dissolved oxygen, pH, sulfite concentration, contaminant types, UV intensity and wavelength). Therefore, more precise reaction conditions are controlled to accurately explore the reaction mechanisms. In addition, a variety of advanced technologies (e.g., *in-situ* Raman techniques, electrochemical characterization and density functional theoretical calculations) is needed to explore intrinsic catalytic sites and reaction mechanisms in-depth.

(6) Most of the sulfite activators currently used is metal ions or powder catalysts, which are difficult to recover during application, resulting in a potential secondary pollution problem. In the future research, more consideration should be given to integrating catalysts into membrane reactors, packed columns or fixed-beds reactors. At the same time, the effectiveness of the sulfite-based AOPs/ARPs in eliminating contaminants from real polluted sites (e.g., surface water and wastewater) should also be evaluated.

(7) The toxicity variation of contaminants during degradation should be assessed, because degradation products may be more toxic than the parent compound. In addition, some undesirable by-products may be produced in complicated water containing different water matrices (e.g., halogen anions, nitrate/nitrite and natural organic matters), which lead to the increased toxicity.

Declaration of Competing Interest

The authors declare that they have no known competing financial interests or personal relationships that could have appeared to influence the work reported in this paper.

Acknowledgements

This work was supported by the National Natural Science Foundation of China (Grant No.: 51978178, 51478172 and 51521006), the Department of Science and Technology of Guangdong Province of China (Contract No.: 2019A1515012044 and 2018S0013), the International S&T Cooperation Program of China (Contract No.: 2015DFG92750), the Natural Science Foundation of Zhejiang Province of China (Grant No.: LY17E080002) and the Department of Science and Technology of Hunan Province of China (Contract No.: 2017JJ2029, 2017SK2362 and 2018JJ3053), and the Startup Fund of Guangdong University of Petrochemical Technology (Contract No.: 2020rc041).

References

[1] Y. Feng, H.H.M. Rijnaarts, D. Yntema, Z. Gong, D.D. Dionysiou, Z. Cao, S. Miao, Y. Chen, Y. Ye, Y. Wang, Applications of anodized TiO_2 nanotube arrays on the removal of aqueous contaminants of emerging concern: A review, Water Res. 186 (2020), 116327.

[2] T. Luo, Y. Peng, L. Chen, J. Li, F. Wu, D. Zhou, Metal-free electro-activated sulfite process for As(III) oxidation in water using graphite electrodes, Environ. Sci. Technol. 54 (2020) 10261–10269.

[3] B. Petrie, R. Barden, B. Kasprzyk-Hordern, A review on emerging contaminants in wastewaters and the environment: Current knowledge, understudied areas and recommendations for future monitoring, Water Res. 72 (2015) 3–27.

[4] N.H. Tran, M. Reinhard, K.Y.H. Gin, Occurrence and fate of emerging contaminants in municipal wastewater treatment plants from different geographical regions-A review, Water Res. 133 (2018) 182–207.

[5] S. Wu, H. He, X. Inthapanya, C. Yang, L. Lu, G. Zeng, Z. Han, Role of biochar on composting of organic wastes and remediation of contaminated soils-a review, Environ. Sci. Pollut. Res. 24 (2017) 16560–16577.

[6] S. Natarajan, H.C. Bajaj, R.J. Tayade, Recent advances based on the synergetic effect of adsorption for removal of dyes from waste water using photocatalytic process, J. Environ. Sci. 65 (2018) 201–222.

[7] Y. He, H. Lin, Z. Guo, W. Zhang, H. Li, W. Huang, Recent developments and advances in boron-doped diamond electrodes for electrochemical oxidation of organic pollutants, Sep. Purif. Technol. 212 (2019) 802–821.

[8] S. Zhang, P. Gu, R. Ma, C. Luo, T. Wen, G. Zhao, W. Cheng, X. Wang, Recent developments in fabrication and structure regulation of visible-light-driven g-C_3N_4-based photocatalysts towards water purification: A critical review, Catal. Today. 335 (2019) 65–77.

[9] G. Yu, Y. Wang, H. Cao, H. Zhao, Y. Xie, Reactive oxygen species and catalytic active sites in heterogeneous catalytic ozonation for water purification, Environ. Sci. Technol. 54 (2020) 5931–5946.

[10] J. Lee, U. von Gunten, J.H. Kim, Persulfate-based advanced oxidation: Critical assessment of opportunities and roadblocks, Environ. Sci. Technol. 54 (2020) 3064–3081.

[11] J. Wang, S. Wang, Activation of persulfate (PS) and peroxymonosulfate (PMS) and application for the degradation of emerging contaminants, Chem. Eng. J. 334 (2018) 1502–1517.

[12] P. Hu, M. Long, Cobalt-catalyzed sulfate radical-based advanced oxidation: a review on heterogeneous catalysts and applications, Appl. Catal. B: Environ. 181 (2016) 103–117.

[13] S. Wu, Y. Lin, C. Yang, C. Du, Q. Teng, Y. Ma, D. Zhang, L. Nie, Y. Zhong, Enhanced activation of peroxymonosulfte by $LaFeO_3$ perovskite supported on Al_2O_3 for degradation of organic pollutants, Chemosphere 237 (2019), 124478.

[14] W.D. Oh, Z. Dong, T.T. Lim, Generation of sulfate radical through heterogeneous catalysis for organic contaminants removal: Current development, challenges and prospects, Appl. Catal. B: Environ. 194 (2016) 169–201.

[15] J. Huang, H. Zhang, Mn-based catalysts for sulfate radical-based advanced oxidation processes: A review, Environ. Int. 133 (2019), 105141.

[16] X. Duan, H. Sun, Z. Shao, S. Wang, Nonradical reactions in environmental remediation processes: Uncertainty and challenges, Appl. Catal. B: Environ. 224 (2018) 973–982.

[17] Y. Lin, H. Liu, C. Yang, X. Wu, C. Du, L. Jiang, Y. Zhong, Gama-graphyne as photogenerated electrons transfer layer enhances photocatalytic performance of silver phosphate, Appl. Catal. B: Environ. 264 (2020), 118479.

[18] R. Li, C. Yang, H. Chen, G. Zeng, G. Yu, J. Guo, Removal of triazophos pesticide from wastewater with Fenton reagent, J. Hazard. Mater. 167 (2009) 1028–1032.

[19] J. Lei, P. Duan, W. Liu, Z. Sun, X. Hu, D Degradation of aqueous cefotaxime in electro-oxidation - electro-Fenton-persulfate system with Ti/CNT/SnO_2-Sb-Er anode and Ni@NCNT cathode, Chemosphere 250 (2020), 126163.

[20] F. Ghanbari, M. Moradi, Application of peroxymonosulfate and its activation methods for degradation of environmental organic pollutants: Review, Chem. Eng. J. 310 (2017) 41–62.

[21] G.P. Anipsitakis, D.D. Dionysiou, Radical generation by the interaction of transition metals with common oxidants, Environ. Sci. Technol. 38 (2004) 3705–3712.

[22] T. Liu, D. Zhang, K. Yin, C. Yang, S. Luo, J.C. Crittenden, Degradation of thiacloprid via unactivated peroxymonosulfate: The overlooked singlet oxygen oxidation, Chem. Eng. J. 388 (2020), 124264.

[23] S. Wu, H. He, X. Li, C. Yang, G. Zeng, B. Wu, S. He, L. Lu, Insights into atrazine degradation by persulfate activation using composite of nanoscale zero-valent iron and graphene: performances and mechanisms, Chem. Eng. J. 341 (2018) 126–136.

[24] S. Wu, H. Liu, C. Yang, X. Li, Y. Lin, K. Yin, J. Sun, Q. Teng, C. Du, Y. Zhong, High-performance porous carbon catalysts doped by iron and nitrogen for degradation of bisphenol F via peroxymonosulfate activation, Chem. Eng. J. 392 (2020), 123683.

[25] X. Chen, W.D. Oh, T.T. Lim, Graphene-and CNTs-based carbocatalysts in persulfates activation: material design and catalytic mechanisms, Chem. Eng. J. 354 (2018) 941–976.

[26] J. Luo, T. Liu, D. Zhang, K. Yin, D. Wang, W. Zhang, C. Liu, C. Yang, Y. Wei, L. Wang, S. Luo, J.C. Crittenden, The individual and Co-exposure degradation of benzophenone derivatives by UV/H_2O_2 and UV/PDS in different water matrices, Water Res. 159 (2019) 102–110.

[27] L. Chen, X. Peng, J. Liu, J. Li, F. Wu, Decolorization of orange II in aqueous solution by an Fe(II)/sulfite system: Replacement of persulfate, Ind. Eng. Chem. 51 (2012) 13632–13638.

[28] M.H. Conklin, M.R. Hoffmann, Metal ion-sulfur(IV) chemistry. 3. Thermodynamics and kinetics of transient iron(III)-sulfur(IV) complexes, Environ. Sci. Technol. 22 (1988) 899–907.

[29] T.E. Graedel, C.J. Weschler, M.L. Mandich, Influence of transition metal complexes on atmospheric droplet acidity, Nature 317 (1985) 240–242.

[30] L.R. Martin, M.W. Hill, The iron catalyzed oxidation of sulfur: Reconciliation of the literature rates, Atmos. Environ. 21 (1967) 1487–1490.

[31] L.R. Martin, M.W. Hill, A.F. Tai, T.W. Good, The iron catalyzed oxidation of sulfur (IV) in aqueous solution: Differing effects of organics at high and low pH, J. Geophys. Res. Atmos. 96 (1991) 3085–3097.

[32] T.N. Das, Reactivity and role of $SO_5^{\bullet -}$ radical in aqueous medium chain oxidation of sulfite to sulfate and atmospheric sulfuric acid generation, J. Phys. Chem. A 105 (2001) 9142–9155.

[33] Y.J. Lee, G.T. Rochelle, Oxidative degradation of organic acid conjugated with sulfite oxidation in flue gas desulfurization: Products, kinetics, and mechanism, Environ. Sci. Technol. 21 (1987) 266–272.

[34] Z. Liu, S. Yang, Y. Yuan, J. Xu, Y. Zhu, J. Li, F. Wu, A novel heterogeneous system for sulfate radical generation through sulfite activation on a $CoFe_2O_4$ nanocatalyst surface, J. Hazard. Mater. 324 (2017) 583–592.

[35] Y. Gu, T. Liu, Q. Zhang, W. Dong, Efficient decomposition of perfluorooctanoic acid by a high photon flux UV/sulfite process: Kinetics and associated toxicity, Chem. Eng. J. 326 (2017) 1125–1133.

[36] P. Xie, L. Zhang, J. Chen, J. Ding, Y. Wan, S. Wang, Z. Wang, A. Zhou, J. Ma, Enhanced degradation of organic contaminants by zero-valent iron sulfite process under simulated sunlight irradiation, Water Res. 149 (2019) 169–178.

[37] C. Guan, J. Jiang, S. Pang, Y. Zhou, Y. Gao, J. Li, Z. Wang, Formation and control of bromate in sulfate radical-based oxidation processes for the treatment of waters containing bromide: A critical review, Water Res. 115725 (2020).

[38] D. Zhou, L. Chen, J. Li, F. Wu, Transition metal catalyzed sulfite auto-oxidation systems for oxidative decontamination in waters: A state-of-the-art minireview, Chem. Eng. J. 346 (2018) 726–738.

[39] P. Xie, Y. Guo, Y. Chen, Z. Wang, R. Shang, S. Wang, J. Ding, Y. Wan, W. Jiang, J. Ma, Application of a novel advanced oxidation process using sulfite and zero-valent iron in treatment of organic pollutants, Chem. Eng. J. 314 (2017) 240–248.

[40] W. Wu, X. Zhao, G. Jing, Z. Zhou, Efficient activation of sulfite autoxidation process with copper oxides for iohexol degradation under mild conditions, Sci. Total. Environ. 695 (2019), 133836.

[41] W. Ding, X. Huang, W. Zhang, F. Wu, J. Li, Sulfite activation by a low-leaching silica-supported copper catalyst for oxidation of As(III) in water at circumneutral pH, Chem. Eng. J. 359 (2019) 1518–1526.

[42] X. Zhao, W. Wu, G. Jing, Z. Zhou, Activation of sulfite autoxidation with $CuFe_2O_4$ prepared by MOF-templated method for abatement of organic contaminants, Environ. Pollut. 260 (2020), 114038.

[43] L.Z. Huang, X. Wei, E. Gao, C. Zhang, X.M. Hu, Y. Chen, Z. Liu, N. Finck, J. Lützenkirchen, D.D. Dionysiou, Single Fe atoms confined in two-dimensional MoS_2 for sulfite activation: A biomimetic approach towards efficient radical generation, Appl. Catal. B: Environ. 268 (2020), 118459.

[44] F. Chen, Q. Yang, F. Yao, Y. Ma, Y. Wang, X. Li, D. Wang, L. Wang, H. Yu, Synergetic transformations of multiple pollutants driven by $BiVO_4$-catalyzed sulfite under visible light irradiation: Reaction kinetics and intrinsic mechanism, Chem. Eng. J. 355 (2019) 624–636.

[45] Y. Bao, S. Deng, X. Jiang, Y. Qu, Y. He, L. Liu, Q. Chai, M. Mumtaz, J. Huang, G. Cagnetta, G. Yu, Degradation of PFOA substitute: GenX (HFPO–DA Ammonium Salt): Oxidation with UV/Persulfate or reduction with UV/Sulfite? Environ. Sci. Technol. 52 (2018) 11728–11734.

[46] K. Yu, X. Li, L. Chen, J. Fang, H. Chen, Q. Li, N. Chi, J. Ma, Mechanism and efficiency of contaminant reduction by hydrated electron in the sulfite/iodide/UV process, Water Res 129 (2018) 357–364.

[47] X. Liu, B.P. Vellanki, B. Batchelor, A. Abdel-Wahab, Degradation of 1,2-dichloroethane with advanced reduction processes (ARPs): Effects of process variables and mechanisms, Chem. Eng. J. 237 (2014) 300–307.

[48] T. Luo, Z. Wang, Y. Wang, Z. Liu, P. Pozdnyakov, Different role of bisulfite/sulfite in UVC-S(IV)-O_2 system for arsenite oxidation in water, Molecules 24 (2019) 2307.

[49] B. Xie, C. Shan, Z. Xu, X. Li, X. Zhang, J. Chen, B. Pan, One-step removal of Cr(VI) at alkaline pH by UV/sulfite process: Reduction to Cr(III) and in situ Cr(III) precipitation, Chem. Eng. J. 308 (2017) 791–797.

[50] X. Wang, H. Liu, C. Shan, W. Zhang, B. Pan, A novel combined process for efficient removal of Se(VI) from sulfate-rich water: Sulfite/UV/Fe(III) coagulation, Chemosphere 211 (2018) 867–874.

[51] V.S.V. Botlaguduru, B. Batchelor, A. Abdel-Wahab, Application of UV–sulfite advanced reduction process to bromate removal, J. Water. Process. Eng. 5 (2015) 76–82.

[52] B.P. Vellanki, B. Batchelor, Perchlorate reduction by the sulfite/ultraviolet light advanced reduction process, J. Hazard. Mater. 262 (2013) 348–356.

[53] J. Cui, P. Gao, Y. Deng, Destruction of per- and polyfluoroalkyl substances (PFAS) with advanced reduction processes (ARPs): A critical review, Environ. Sci. Technol. 54 (2020) 3752–3766.

[54] Z. Song, H. Tang, N. Wang, L. Zhu, Reductive defluorination of perfluorooctanoic acid by hydrated electrons in a sulfite-mediated UV photochemical system, J. Hazard. Mater. 262 (2013) 332–338.

[55] T. Zhang, J. Wang, D. Yan, L. Wang, X. Liu, Efficient reduction of bromate by iodide-assisted UV/sulfite process, Catalysts 8 (2018) 652.

[56] L. Wang, X. Liu, Fast degradation of monochloroacetic acid by BiOI-enhanced UV/S(IV) process: Efficiency and mechanism, Catalysts 9 (2019) 460.

[57] A. Kotronarou, L. Sigg, Sulfur dioxide oxidation in atmospheric water: Role of iron(II) and effect of ligands, Environ. Sci. Technol. 27 (1993) 2725–2735.

[58] J. Ziajka, F. Beer, P. Warneck, Iron-catalysed oxidation of bisulphite aqueous solution: Evidence for a free radical chain mechanism, Atmos. Environ. 28 (1994) 2549–2552.

[59] P. Warneck, J. Ziajka, Reaction mechanism of the iron(III)-catalyzed autoxidation of bisulfite in aqueous solution: Steady state description for benzene as radical scavenger, Berichte der Bunsengesellschaft für Physikalische Chemie 99 (1995) 59–65.

[60] H. Dong, G. Wei, D. Yin, X. Guan, Mechanistic insight into the generation of reactive oxygen species in sulfite activation with Fe(III) for contaminants degradation, J. Hazard. Mater. 384 (2020), 121497.

[61] M. Luo, H. Wang, Y. Zhang, Y. Zhong, K. Wang, Surface treatment by the Fe(III)/sulfite system for flotation separation of hazardous chlorinated plastics from the mixed waste plastics, J. Hazard. Mater. 377 (2019) 34–41.

[62] H. Wang, S. Wang, Y. Liu, Y. Fu, P. Wu, G. Zhou, Degradation of diclofenac by Fe (II)-activated bisulfite: Kinetics, mechanism and transformation products, Chemosphere 237 (2019), 124518.

[63] C. Brandt, I. Fabian, R. van Eldik, Kinetics and mechanism of the iron(III)-catalyzed autoxidation of sulfur(IV) oxides in aqueous solution. Evidence for the redox cycling of iron in the presence of oxygen and modeling of the overall reaction mechanism, Inorg. Chem 33 (1994) 687–701.

[64] G.V. Buxton, S. McGowan, G.A. Salmon, J.E. Williams, N.D. Wood, A study of the spectra and reactivity of oxysulphur-radical anions involved in the chain oxidation of S(IV): A pulse and γ-radiolysis study, Atmos. Environ 30 (1996) 2483–2493.

[65] M. Fischer, P. Warneck, Photodecomposition and photooxidation of hydrogen sulfite in aqueous solution, J. Phys. Chem. 100 (1996) 15111–15117.

[66] R.E. Huie, P. Neta, One-electron redox reactions in aqueous solutions of sulfite with hydroquinone and other hydroxyphenols, J. Phys. Chem. 89 (1985) 3918–3921.

[67] Y. Yuan, T. Luo, J. Xu, J. Li, F. Wu, M. Brigante, G. Mailhot, Enhanced oxidation of aniline using Fe(III)-S(IV) system: Role of different oxysulfur radicals, Chem. Eng. J. 362 (2019) 183–189.

[68] X. Chen, W. Miao, Y. Yang, S. Hao, S. Mao, Aeration-assisted sulfite activation with ferrous for enhanced chloramphenicol degradation, Chemosphere 238 (2020), 124599.

[69] D. Li, D. Chen, Y. Yao, J. Lin, F. Gong, L. Wang, L. Luo, Z. Huang, L. Zhang, Strong enhancement of dye removal through addition of sulfite to persulfate activated by a supported ferric citrate catalyst, Chem. Eng. J. 288 (2016) 806–812.

[70] Y. Yu, S. Li, X. Peng, S. Yang, Y. Zhu, L. Chen, F. Wu, G. Mailhot, Efficient oxidation of bisphenol A with oxysulfur radicals generated by iron-catalyzed autoxidation of sulfite at circumneutral pH under UV irradiation, Environ. Chem. Lett. 14 (2016) 527–532.

[71] G. Lente, I. Fábián, Kinetics and mechanism of the oxidation of sulfur(IV) by iron (III) at metal ion excess, J. Chem. Soc. Dalton. Trans. 5 (2002) 778–784.

[72] D. Zhou, L. Chen, C. Zhang, Y. Yu, L. Zhang, F. Wu, A novel photochemical system of ferrous sulfite complex: Kinetics and mechanisms of rapid decolorization of Acid Orange 7 in aqueous solutions, Water Res. 57 (2014) 87–95.

[73] Y. Guo, X. Lou, C. Fang, D. Xiao, Z. Wang, J. Liu, Novel photo-sulfite system: Toward simultaneous transformations of inorganic and organic pollutants, Environ. Sci. Technol. 47 (2013) 11174–11181.

[74] J. Xu, W. Ding, F. Wu, G. Mailhot, D. Zhou, K. Hanna, Rapid catalytic oxidation of arsenite to arsenate in an iron(III)/sulfite system under visible light, Appl. Catal. B: Environ. 186 (2016) 56–61.

[75] L. Zhang, L. Chen, M. Xiao, L. Zhang, F. Wu, L. Ge, Enhanced decolorization of orange II solutions by the Fe(II)–sulfite system under Xenon lamp irradiation, Ind. Eng. Chem. Res. 52 (2013) 10089–10094.

[76] Y. Zuo, J. Zhan, T. Wu, Effects of monochromatic UV-Visible light and sunlight on Fe(III)-catalyzed oxidation of dissolved sulfur dioxide, J. Atmos. Chem. 50 (2005) 195–210.

[77] V.K. Sharma, R. Zboril, R.S. Varma, Ferrates: Greener oxidants with multimodal action in water treatment technologies, Acc. Chem. Res. 48 (2015) 182–191.

[78] S. Wu, H. Li, X. Li, H. He, C. Yang, Performances and mechanisms of efficient degradation of atrazine using peroxymonosulfate and ferrate as oxidants, Chem. Eng. J. 353 (2018) 533–541.

[79] S. Wu, H. Liu, Y. Lin, C. Yang, W. Lou, J. Sun, C. Du, D. Zhang, L. Nie, K. Yin, Y. Zhong, Insights into mechanisms of UV/ferrate oxidation for degradation of phenolic pollutants: Role of superoxide radicals, Chemosphere 244 (2020), 125490.

[80] M. Feng, C. Jinadatha, T.J. McDonald, V.K. Sharma, Accelerated oxidation of organic contaminants by ferrate(VI): The overlooked role of reducing additives, Environ. Sci. Technol. 52 (2018) 11319–11327.

[81] J. Zhang, L. Zhu, Z. Shi, Y. Gao, Rapid removal of organic pollutants by activation sulfite with ferrate, Chemosphere 186 (2017) 576–579.

[82] A. Acosta-Rangel, M. Sánchez-Polo, M. Rozalen, J. Rivera-Utrilla, A.M.S. Polo, A. J. Mota, Comparative study of the oxidative degradation of different 4-amino-benzene sulfonamides in aqueous solution by sulfite activation in the presence of Fe(0), Fe(II), Fe(III) or Fe(VI), Water 11 (2019) 2332.

[83] S. Sun, S. Pang, J. Jiang, J. Ma, Z. Huang, J. Zhang, Y. Liu, C. Xu, Q. Liu, Y. Yuan, The combination of ferrate(VI) and sulfite as a novel advanced oxidation process for enhanced degradation of organic contaminants, Chem. Eng. J. 333 (2018) 11–19.

[84] B. Sun, X. Guan, J. Fang, P.G. Tratnyek, Activation of manganese oxidants with bisulfite for enhanced oxidation of organic contaminants: The involvement of Mn (III), Environ. Sci. Technol. 49 (2015) 12414–12421.

[85] M. Sun, W. Huang, H. Cheng, J. Ma, Y. Kong, S. Komarneni, Degradation of dye in wastewater by homogeneous Fe(VI)/$NaHSO_3$ system, Chemosphere 228 (2019) 595–601.

[86] M. Feng, V.K. Sharma, Enhanced oxidation of antibiotics by ferrate(VI)-sulfur(IV) system: Elucidating multi-oxidant mechanism, Chem. Eng. J. 341 (2018) 137–145.

[87] B. Shao, H. Dong, B. Sun, X. Guan, Role of ferrate(IV) and ferrate(V) in activating ferrate(VI) by calcium sulfite for enhanced oxidation of organic contaminants, Environ. Sci. Technol. 53 (2019) 894–902.

[88] V.K. Sharma, Ferrate(V) oxidation of pollutants: A premix pulse radiolysis study, Radiat. Phys. Chem. 65 (2002) 349–355.

[89] B. Shao, H. Dong, L. Feng, J. Qiao, X. Guan, Influence of [sulfite]/[Fe(VI)] molar ratio on the active oxidants generation in Fe(VI)/sulfite process, J. Hazard. Mater. 384 (2020), 121303.

[90] B.M. Bzdyra, C.D. Spellman, I. Andreu, J.E. Goodwill, Sulfite activation changes character of ferrate resultant particles, Chem. Eng. J. 393 (2020), 124771.

[91] X. Zhao, W. Wu, Y. Yan, Efficient abatement of an iodinated X-ray contrast media iohexol by Co(II) or Cu(II) activated sulfite autoxidation process, Environ. Sci. Pollut. Res. 26 (2019) 24707–24719.

[92] Y. Yuan, D. Zhao, J. Li, F. Wu, M. Brigante, G. Mailhot, Rapid oxidation of paracetamol by Cobalt(II) catalyzed sulfite at alkaline pH, Catal. Today. 313 (2018) 155–160.

[93] W. Pasiuk-Bronikowska, T. Bronikowski, M. Ulejczyk, Mechanism and kinetics of autoxidation of calcium sulfite slurries, Environ. Sci. Technol. 26 (1992) 1976–1981.

[94] L. Chen, X. Huang, M. Tang, D. Zhou, F. Wu, Rapid dephosphorylation of glyphosate by Cu-catalyzed sulfite oxidation involving sulfate and hydroxyl radicals, Environ. Chem. Lett. 16 (2018) 1507–1511.

[95] L. Chen, M. Tang, C. Chen, M. Chen, K. Luo, J. Xu, D. Zhou, F. Wu, Efficient bacterial inactivation by transition metal catalyzed auto-oxidation of sulfite, Environ. Sci. Technol. 51 (2017) 12663–12671.

[96] L. Jia, X. Pei, F. Yang, Electrolysis-assisted Mn(II)/sulfite process for organic contaminant degradation at near-neutral pH, Water 11 (2019) 1608.

[97] J. Zhang, J. Ma, H. Song, S. Sun, Z. Zhang, T. Yang, Organic contaminants degradation from the S(IV) autoxidation process catalyzed by ferrous-manganous ions: A noticeable Mn(III) oxidation process, Water Res. 133 (2018) 227–235.

[98] J. Berglund, S. Fronaeus, L.I. Elding, Kinetics and mechanism for manganese-catalyzed oxidation of sulfur (IV) by oxygen in aqueous solution, Inorg. Chem. 32 (1993) 4527–4538.

[99] D. Rao, Y. Sun, B. Shao, J. Qiao, X. Guan, Activation of oxygen with sulfite for enhanced removal of Mn(II): The involvement of $SO_4^{\bullet-}$, Water Res. 157 (2019) 435–444.

[100] B. Sun, H. Dong, D. He, D. Rao, X. Guan, Modeling the kinetics of contaminants oxidation and the generation of manganese(III) in the permanganate/bisulfite process, Environ. Sci. Technol. 50 (2016) 1473–1482.

[101] B. Sun, D. Li, W. Linghu, X. Guan, Degradation of ciprofloxacin by manganese(III) intermediate: Insight into the potential application of permanganate/bisulfite process, Chem. Eng. J. 339 (2018) 144–152.

[102] W. Li, Y. Lou, A. Fang, K. Feng, D. Xing, Potassium permanganate ($KMnO_4$)/ sodium sulfite (Na_2SO_3) rapidly disintegrates waste activated sludge by reactive Mn(III) species and shapes microbial community structure, Chem. Eng. J. 394 (2020), 124920.

[103] Z. Shi, C. Jin, J. Zhang, L. Zhu, Insight into mechanism of arsanilic acid degradation in permanganate-sulfite system: Role of reactive species, Chem. Eng. J. 359 (2019) 1463–1471.

[104] S. Duan, P. Hou, X. Yuan, Z. Qiang, H. Dong, Homogeneous activation of bisulfite by transition metals for micro-pollutant degradation: Mn(VII) versus Cr(VI), Chem. Eng. J. 124814 (2020).

[105] C.E. Barrera-Díaz, V. Lugo-Lugo, B. Bilyeu, A review of chemical, electrochemical and biological methods for aqueous Cr(VI) reduction, J. Hazard. Mater. 223–224 (2012) 1–12.

[106] X. Li, W.L. Yang, H. He, S. Wu, Q. Zhou, C. Yang, G. Zeng, L. Luo, W. Lou, Responses of microalgae *Coelastrella* sp. to stress of cupric ions in treatment of anaerobically digested swine wastewater, Bioresour. Technol. 251 (2018) 274–279.

[107] B. Jiang, Y. Liu, J. Zheng, M. Tan, Z. Wang, M. Wu, Synergetic transformations of multiple pollutants driven by Cr(VI)–sulfite reactions, Environ. Sci. Technol. 49 (2015) 12363–12371.

[108] Y. Yuan, S. Yang, D. Zhou, F. Wu, A simple Cr(VI)-S(IV)-O_2 system for rapid and simultaneous reduction of Cr(VI) and oxidative degradation of organic pollutants, J Hazard Mater. 307 (2016) 294–301.

[109] H. Dong, G. Wei, T. Cao, B. Shao, X. Guan, T.J. Strathmann, Insights into the oxidation of organic cocontaminants during Cr(VI) reduction by sulfite: The overlooked significance of Cr(V), Environ. Sci. Technol. 54 (2020) 1157–1166.

[110] G.P. Haight, E. Perchonock, F. Emmenegger, G. Gordon, The mechanism of the oxidation of sulfur(IV) by chromium (VI) in acid solution1, J. Am. Chem. Soc. 87 (1965) 3835–3840.

[111] H. Dong, G. Wei, W. Fan, S. Ma, H. Zhao, W. Zhang, X. Guan, T.J. Strathmann, Reinvestigating the role of reactive species in the oxidation of organic co-contaminants during Cr(VI) reactions with sulfite, Chemosphere 196 (2018) 593–597.

[112] Y. Gao, H.P. Pan, Y. Zhou, Z. Wang, S.Y. Pang, C.T. Guan, Y.M. Shen, J. Jiang, Are free radicals actually responsible for enhanced oxidation of contaminants by Cr (VI) in the presence of bisulfite? Chemosphere 248 (2020), 126000.

[113] B. Jiang, S. Xin, Y. Liu, H. He, L. Li, Y. Tang, S. Luo, X. Bi, The role of thiocyanate in enhancing the process of sulfite reducing Cr(VI) by inhibiting the formation of reactive oxygen species, J. Hazard. Mater. 343 (2018) 1–9.

[114] B. Jiang, X. Wang, Y. Liu, Z. Wang, J. Zheng, M. Wu, The roles of polycarboxylates in Cr(VI)/sulfite reaction system: Involvement of reactive oxygen species and intramolecular electron transfer, J. Hazard. Mater. 304 (2016) 457–466.

[115] A.A. Ensafi, E. Heydari-Bafrooei, B. Rezaei, DNA-based biosensor for comparative study of catalytic effect of transition metals on autoxidation of sulfite, Anal. Chem. 85 (2013) 991–997.

[116] Y. Zou, X. Wang, A. Khan, P. Wang, Y. Liu, A. Alsaedi, T. Hayat, X. Wang, Environmental remediation and application of nanoscale zero-valent iron and its composites for the removal of heavy metal ions: A review, Environ. Sci. Technol. 50 (2016) 7290–7304.

[117] S. Bae, R.N. Collins, T.D. Waite, K. Hanna, Advances in surface passivation of nanoscale zerovalent iron: A critical review, Environ. Sci. Technol. 52 (2018) 12010–12025.

[118] Y. Liu, J. Wang, Reduction of nitrate by zero valent iron (ZVI)-based materials: A review, Sci. Total. Environ. 671 (2019) 388–403.

[119] X. Xiong, J. Gan, W. Zhan, B. Sun, Effects of oxygen and weak magnetic field on Fe^0/bisulfite system: performance and mechanisms, Environ. Sci. Pollut. Res. 23 (2016) 16761–16770.

[120] J. Du, W. Guo, H. Wang, R. Yin, H. Zheng, X. Feng, D. Che, N. Ren, Hydroxyl radical dominated degradation of aquatic sulfamethoxazole by Fe^0/bisulfite/O_2: Kinetics, mechanisms, and pathways, Water Res. 138 (2018) 323–332.

[121] Y. Yang, M. Sun, J. Zhou, J. Ma, S. Komarneni, Degradation of orange II by Fe@ Fe_2O_3 core shell nanomaterials assisted by $NaHSO_3$, Chemosphere 244 (2020), 125588.

[122] J. Xu, X. Wang, F. Pan, Y. Qin, J. Xia, J. Li, F. Wu, Synthesis of the mesoporous carbon-nano-zero-valent iron composite and activation of sulfite for removal of organic pollutants, Chem. Eng. J. 353 (2018) 542–549.

[123] X. Zhao, Y. Wu, D. Xing, Z. Ren, L. Ye, Enhanced abatement of organic contaminants by zero-valent copper and sulfite, Environ. Chem. Lett. 18 (2020) 237–241.

[124] Y. Mei, J. Zeng, M. Sun, J. Ma, S. Komarneni, A novel Fenton-like system of Fe_2O_3 and $NaHSO_3$ for Orange II degradation, Sep. Purif. Technol. 230 (2020), 115866.

[125] S.R. Zhu, J.N. Yang, Y. Liu, W. Gao, X. Yi, H. Zhou, M. Wu, Synergetic interaction of lithium cobalt oxide with sulfite to accelerate the degradation of organic aqueous pollutants, Mater. Chem. Phys. 249 (2020), 123123.

[126] W. Ding, W. Xiao, W. Huang, Q. Sun, H. Zheng, Sulfite activation on a silica-supported well-dispersed cobalt catalyst via an electron transfer complex path, J. Clean. Prod. 257 (2020), 120457.

[127] L. Chen, T. Luo, S. Yang, J. Xu, Z. Liu, F. Wu, Efficient metoprolol degradation by heterogeneous copper ferrite/sulfite reaction, Environ. Chem. Lett. 16 (2018) 599–603.

[128] Y. Chen, M. Li, Y. Tong, Z. Liu, L. Fang, Y. Wu, Z. Fang, F. Wu, L.Z. Huang, Radical generation via sulfite activation on $NiFe_2O_4$ surface for estriol removal: Performance and mechanistic studies, Chem. Eng. J. 368 (2019) 495–503.

[129] Y. Huang, C. Han, Y. Liu, M.N. Nadagouda, L. Machala, K.E. O'Shea, V.K. Sharma, Degradation of atrazine by $Zn_xCu_{1-x}Fe_2O_4$ nanomaterial-catalyzed sulfite under UV–vis light irradiation: Green strategy to generate $SO_4^{\bullet-}$, Appl. Catal. B: Environ. 221 (2018) 380–392.

[130] R. Dou, H. Cheng, J. Ma, S. Komarneni, Manganese doped magnetic cobalt ferrite nanoparticles for dye degradation via a novel heterogeneous chemical catalysis, Mater. Chem. Phys. 240 (2020), 122181.

[131] Y. Chen, Y. Tong, Y. Xue, Z. Liu, M. Tang, L.-Z. Huang, S. Shao, Z. Fang, Degradation of the β-blocker propranolol by sulfite activation using FeS, Chem. Eng. J. 385 (2020), 123884.

[132] X. Fan, Y. Zhou, G. Zhang, T. Liu, W. Dong, In situ photoelectrochemical activation of sulfite by MoS_2 photoanode for enhanced removal of ammonium nitrogen from wastewater, Appl. Catal. B: Environ. 244 (2019) 396–406.

[133] Y. Qu, X. Song, X. Chen, X. Fan, G. Zhang, Tuning charge transfer process of MoS_2 photoanode for enhanced photoelectrochemical conversion of ammonia in water into gaseous nitrogen, Chem. Eng. J. 382 (2020), 123048.

[134] J. Cao, W. Nie, L. Huang, Y. Ding, K. Lv, H. Tang, Photocatalytic activation of sulfite by nitrogen vacancy modified graphitic carbon nitride for efficient degradation of carbamazepine, Appl. Catal. B: Environ. 241 (2019) 18–27.

[135] W. Deng, H. Zhao, F. Pan, X. Feng, B. Jung, A. Abdel-Wahab, B. Batchelor, Y. Li, Visible-light-driven photocatalytic degradation of organic water pollutants promoted by sulfite addition, Environ. Sci. Technol. 51 (2017) 13372–13379.

[136] B. Jung, W. Deng, Y. Li, B. Batchelor, A. Abdel-Wahab, Simulated solar light-driven photocatalytic degradation of trichloroethylene in water using BiOBr promoted by sulfite addition, Environ. Sci. Eur. 32 (2020) 8.

[137] A.U.R. Bacha, H. Cheng, J. Han, I. Nabi, K. Li, T. Wang, Y. Yang, S. Ajmal, Y. Liu, L. Zhang, Significantly accelerated PEC degradation of organic pollutant with addition of sulfite and mechanism study, Appl. Catal. B: Environ. 248 (2019) 441–449.

[138] Y. Lin, C. Yang, S. Wu, X. Li, Y. Chen, W. Yang, Construction of built-in electric field within silver phosphate photocatalyst for enhanced removal of recalcitrant organic pollutants, Adv. Funct. Mater. 30 (2020) 2002918.

[139] Y. Lin, X. Wu, Y. Han, C. Yang, Y. Ma, C. Du, Q. Teng, H. Liu, Y. Zhong, Spatial separation of photogenerated carriers and enhanced photocatalytic performance on Ag_3PO_4 catalysts via coupling with PPy and MWCNTs, Appl. Catal. B: Environ. 258 (2019), 117969.

[140] L. Chen, W. Ding, F. Wu, Comment on “Visible-light-driven photocatalytic degradation of organic water pollutants promoted by sulfite addition”, Environ. Sci. Technol. 52 (2018) 1675–1676.

[141] J.A. Khan, M. Sayed, N.S. Shah, S. Khan, Y. Zhang, G. Boczkaj, H.M. Khan, D. D. Dionysiou, Synthesis of eosin modified TiO2 film with co-exposed 001 and 101 facets for photocatalytic degradation of para-aminobenzoic acid and solar H2 production, Appl. Catal. B: Environ. 265 (2020), 118557.

[142] Y. Wei, Q. Zou, P. Ye, M. Wang, X. Li, A. Xu, Photocatalytic degradation of organic pollutants in wastewater with g-C_3N_4/sulfite system under visible light irradiation, Chemosphere 208 (2018) 358–365.

[143] G. Li, C. Wang, Y. Yan, X. Yan, W. Li, X. Feng, J. Li, Q. Xiang, W. Tan, F. Liu, H. Yin, Highly enhanced degradation of organic pollutants in hematite/sulfite/photo system, Chem. Eng. J. 386 (2020), 124007.

[144] A. Abdelhaleem, W. Chu, X. Liang, Diphenamid degradation via sulfite activation under visible LED using Fe (III) impregnated N-doped TiO_2 photocatalyst, Appl. Catal. B: Environ. 244 (2019) 823–835.

[145] X. Yu, D. Cabooter, R. Dewil, Efficiency and mechanism of diclofenac degradation by sulfite/UV advanced reduction processes (ARPs), Sci. Total. Environ. 688 (2019) 65–74.

[146] B. Jung, H. Farzaneh, A. Khodary, A. Abdel-Wahab, Photochemical degradation of trichloroethylene by sulfite-mediated UV irradiation, J. Environ. Chem. Eng. 3 (2015) 2194–2202.

[147] S. Ding, F. Wang, W. Chu, Z. Cao, Y. Pan, N. Gao, Rapid degradation of brominated and iodinated haloacetamides with sulfite in drinking water: Degradation kinetics and mechanisms, Water Res. 143 (2018) 325–333.

[148] W.A. MacCrehan, J.S. Jensen, G.R. Helz, Detection of sewage organic chlorination products that are resistant to dechlorination with sulfite, Environ. Sci. Technol. 32 (1998) 3640–3645.

[149] X. Li, J. Ma, G. Liu, J. Fang, S. Yue, Y. Guan, L. Chen, X. Liu, Efficient reductive dechlorination of monochloroacetic Acid by Sulfite/UV process, Environ. Sci. Technol. 46 (2012) 7342–7349.

[150] K. Hara, K. Sayama, H. Arakawa, UV photoinduced reduction of water to hydrogen in Na_2S, Na_2SO_3, and $Na_2S_2O_4$ aqueous solutions, J. Photoch. Photobio A: Chem. 128 (1999) 27–31.

[151] X. Yu, D. Cabooter, R. Dewil, Effects of process variables and kinetics on the degradation of 2,4-dichlorophenol using advanced reduction processes (ARP), J. Hazard. Mater. 357 (2018) 81–88.

[152] M.C. Sauer, R.A. Crowell, I.A. Shkrob, Electron photodetachment from aqueous anions. 1. Quantum yields for generation of hydrated electron by 193 and 248 nm laser photoexcitation of miscellaneous inorganic anions, J. Phys. Chem. A. 108 (2004) 5490–5502.

[153] M.G. Gonzalez, E. Oliveros, M. Wörner, A.M. Braun, Vacuum-ultraviolet photolysis of aqueous reaction systems, J. Photoch. Photobio. C: Photoch Rev. 5 (2004) 225–246.

[154] K. Zoschke, H. Börnick, E. Worch, Vacuum-UV radiation at 185 nm in water treatment-A review, Water Res. 52 (2014) 131–145.

[155] X. Liu, T. Zhang, Y. Shao, Aqueous bromate reduction by UV activation of sulfite, CLEAN-Soil Air Water 42 (2014) 1370–1375.

[156] Q. Xiao, S. Yu, L. Li, T. Wang, X. Liao, Y. Ye, An overview of advanced reduction processes for bromate removal from drinking water: Reducing agents, activation methods, applications and mechanisms, J. Hazard. Mater. 324 (2017) 230–240.

[157] Y. Duan, B. Batchelor, Impacts of natural organic matter on perchlorate removal by an advanced reduction process, J. Environ. Sci. Health, Part A 49 (2014) 731–740.

[158] B.P. Vellanki, B. Batchelor, A. Abdel-Wahab, Advanced reduction processes: A new class of treatment processes, Environ. Eng. Sci. 30 (2013) 264–271.

[159] S. Yoon, D.S. Han, X. Liu, B. Batchelor, A. Abdel-Wahab, Degradation of 1,2-dichloroethane using advanced reduction processes, J. Environ. Chem. Eng. 2 (2014) 731–737.

[160] C. Schweitzer, R. Schmidt, Physical mechanisms of generation and deactivation of singlet oxygen, Chem. Rev. 103 (2003) 1685–1757.

[161] Y. Gu, W. Dong, C. Luo, T. Liu, Efficient reductive decomposition of perfluorooctanesulfonate in a high photon flux UV/sulfite system, Environ. Sci. Technol. 50 (2016) 10554–10561.

[162] Z. Lou, J. Xu, J. Zhou, K. Yang, Z. Cao, Y. Li, Y. Liu, L. Lou, X. Xu, Insight into atomic H* generation, H_2 evolution, and cathode potential of MnO_2 induced Pd/Ni foam cathode for electrocatalytic hydrodechlorination, Chem. Eng. J. 374 (2019) 211–220.

[163] Z. Lou, Z. Wang, J. Zhou, C. Zhou, J. Xu, X. Xu, Pd/TiC/Ti electrode with enhanced atomic H* generation, atomic H* adsorption and 2,4-DCBA adsorption for facilitating electrocatalytic hydrodechlorination, Environ. Sci: Nano. 7 (2020) 1566–1581.

[164] G.V. Buxton, C.L. Greenstock, W.P. Helman, A.B. Ross, Critical review of rate constants for reactions of hydrated electrons, hydrogen atoms and hydroxyl radicals ($\bullet OH/{}^{\bullet}O^{-}$) in aqueous solution, J. Phys. Chem. Ref. Data 17 (1988) 513–886.

[165] L. Long, Y. Bu, B. Chen, R. Sadiq, Removal of urea from swimming pool water by UV/VUV: The roles of additives, mechanisms, influencing factors, and reaction products, Water Res. 161 (2019) 89–97.

[166] R.H. Schuler, P. Neta, R.W. Fessenden, Electron spin resonance study of the rate constants for reaction of hydrogen atoms with organic compounds in aqueous solution, J. Phys. Chem. 75 (1971) 1654–1666.

[167] E.J. Hart, E.M. Fielden, M. Anbar, Reactions of carbonylic compounds with hydrated electrons, J. Phys. Chem. 71 (1967) 3993–3998.

[168] X. Liu, S. Yoon, B. Batchelor, A. Abdel-Wahab, Degradation of vinyl chloride (VC) by the sulfite/UV advanced reduction process (ARP): Effects of process variables and a kinetic model, Sci. Total. Environ. 454–455 (2013) 578–583.

[169] G. Matafonova, V. Batoev, Recent advances in application of UV light-emitting diodes for degrading organic pollutants in water through advanced oxidation processes: A review, Water Res. 132 (2018) 177–189.

[170] R. Yin, P. Shen, Z. Lu, A green approach for the reduction of graphene oxide by the ultraviolet/sulfite process, J Colloid. Interf. Sci. 550 (2019) 110–116.

[171] B. Jung, R. Nicola, B. Batchelor, A. Abdel-Wahab, Effect of low- and medium-pressure Hg UV irradiation on bromate removal in advanced reduction process, Chemosphere 117 (2014) 663–672.

[172] B. Xie, X. Li, X. Huang, Z. Xu, W. Zhang, B. Pan, Enhanced debromination of 4-bromophenol by the UV/sulfite process: Efficiency and mechanism, J. Environ. Sci.-China 54 (2017) 231–238.

[173] Y. Tian, W. Shen, F. Jia, Z. Ai, L. Zhang, Sulfite promoted photochemical cleavage of s-triazine ring: The case study of atrazine, Chem. Eng. J. 330 (2017) 1075–1081.

[174] Q. Xiao, Y. Ren, S. Yu, Pilot study on bromate reduction from drinking water by UV/sulfite systems: Economic cost comparisons, effects of environmental parameters and mechanisms, Chem. Eng. J. 330 (2017) 1203–1210.

[175] Q. Xiao, T. Wang, S. Yu, P. Yi, L. Li, Influence of UV lamp, sulfur(IV) concentration, and pH on bromate degradation in UV/sulfite systems: Mechanisms and applications, Water Res. 111 (2017) 288–296.

[176] X. Li, J. Fang, G. Liu, S. Zhang, B. Pan, J. Ma, Kinetics and efficiency of the hydrated electron-induced dehalogenation by the sulfite/UV process, Water Res. 62 (2014) 220–228.

[177] A. Sheikhmohammadi, A. Yazdanbakhsh, G. Moussavi, A. Eslami, M. Rafiee, M. Sardar, M. Almasian, Degradation and COD removal of trichlorophenol from wastewater using sulfite anion radicals in a photochemical process combined with a biological reactor: Mechanisms, degradation pathway, optimization and energy consumption, Process. Saf. Environ. 123 (2019) 263–271.

[178] X. Zhao, D. Cao, P. Su, X. Guan, Efficient recovery of Sb(V) by hydrated electron reduction followed by cathodic deposition in a photoelectrochemical process, Chem. Eng. J. 395 (2020), 124153.

[179] H. Azarpira, M. Abtahi, M. Sadani, S. Rezaei, Z. Atafar, A. Bay, S.M. Mohseni, M. Sarkhosh, M. Shanbedi, H. Alidadi, Y. Fakhri, H. Keramati, V. Fanai, Photocatalytic degradation of trichlorophenol with UV/sulfite/ZnO process, simultaneous usage of homogeneous reductive and heterogeneous oxidative agents generator as a new approach of Advanced Oxidation/Reduction Processes (AO/RPs), J. Photoch. Photobio A: Chem. 374 (2019) 43–51.

[180] M. Entezari, H. Godini, A. Sheikhmohammadi, A. Esrafili, Enhanced degradation of polychlorinated biphenyls with simultaneous usage of reductive and oxidative agents over UV/sulfite/TiO_2 process as a new approach of advanced oxidation/reduction processes, J. Water. Process. Eng. 32 (2019), 100983.

[181] J. Qiao, L. Feng, H. Dong, Z. Zhao, X. Guan, Overlooked role of sulfur-centered radicals during bromate reduction by sulfite, Environ. Sci. Technol. 53 (2019) 10320–10328.

[182] Y. Cao, W. Qiu, J. Li, Y. Zhao, J. Jiang, S. Pang, Sulfite enhanced transformation of iopamidol by UV photolysis in the presence of oxygen: Role of oxysulfur radicals, Water Res. 189 (2021), 116625.

[183] Y. Cao, W. Qiu, J. Li, J. Jiang, S. Pang, Review on UV/sulfite process for water and wastewater treatments in the presence or absence of O_2, Sci. Total Environ. (2020), 142762.

[184] M.G. Seid, K. Cho, S.W. Hong, UV/sulfite chemistry to reduce N-nitrosodimethylamine formation in chlor(am)inated water, Water Res. 185 (2020), 116243.

[185] Y. Gu, T. Liu, H. Wang, H. Han, W. Dong, Hydrated electron based decomposition of perfluorooctane sulfonate (PFOS) in the VUV/sulfite system, Sci. Total. Environ. 607–608 (2017) 541–548.

[186] X. Yu, Z. Gocze, D. Cabooter, R. Dewil, Efficient reduction of carbamazepine using UV-activated sulfite: Assessment of critical process parameters and elucidation of radicals involved, Chem. Eng. J. 404 (2021), 126403.

[187] G.P. Anipsitakis, D.D. Dionysiou, M.A. Gonzalez, Cobalt-mediated activation of peroxymonosulfate and sulfate radical attack on phenolic compounds. Implications of chloride ions, Environ. Sci. Technol. 40 (2006) 1000–1007.

[188] S. Nawaz, N.S. Shah, J.A. Khan, M. Sayed, A.A.H. Al-Muhtaseb, H.R. Andersen, N. Muhammad, B. Murtaza, H.M. Khan, Removal efficiency and economic cost

comparison of hydrated electron-mediated reductive pathways for treatment of bromate, Chem. Eng. J. 320 (2017) 523–531.

[189] D. Wu, P. Ye, M. Wang, Y. Wei, X. Li, A. Xu, Cobalt nanoparticles encapsulated in nitrogen-rich carbon nanotubes as efficient catalysts for organic pollutants degradation via sulfite activation, J. Hazard. Mater. 352 (2018) 148–156.

[190] H.V. Lutze, S. Bircher, I. Rapp, N. Kerlin, R. Bakkour, M. Geisler, C. von Sonntag, T.C. Schmidt, Degradation of chlorotriazine pesticides by sulfate radicals and the influence of organic matter, Environ. Sci. Technol. 49 (2015) 1673–1680.

[191] Q. Zhou, X. Li, Y. Lin, C. Yang, W. Tang, S. Wu, D. Li, W. Lou, Effects of copper ions on removal of nutrients from swine wastewater and on release of dissolved organic matter in duckweed systems, Water Res. 158 (2019) 171–181.

[192] B. Jung, A. Safan, V.S.V. Botlaguduru, B. Batchelor, A. Abdel-Wahab, Impact of natural organic matter on bromate removal in the sulfite/UV-L advanced reduction process, Water. Sci. Technol.-W Sup. 17 (2016) 461–471.

[193] Y. Lin, S. Wu, C. Yang, M. Chen, X. Li, Preparation of size-controlled silver phosphate catalysts and their enhanced photocatalysis performance via synergetic effect with MWCNTs and PANI, Appl. Catal. B: Environ. 245 (2019) 71–86.

[194] S. Wacławek, H.V. Lutze, K. Grübel, V.V.T. Padil, M. Černík, D.D. Dionysiou, Chemistry of persulfates in water and wastewater treatment: A review, Chem. Eng. J. 330 (2017) 44–62.

[195] R. Xiao, Z. Luo, Z. Wei, S. Luo, R. Spinney, W. Yang, D.D. Dionysiou, Activation of peroxymonosulfate/persulfate by nanomaterials for sulfate radical-based advanced oxidation technologies, Curr. Opin. Chem. Eng. 19 (2018) 51–58.

[196] P. Neta, R.E. Huie, A.B. Ross, Rate constants for reactions of inorganic radicals in aqueous solution, J. Phys. Chem. Ref. Data. 17 (1988) 1027–1284.

[197] E. Hayon, A. Treinin, J. Wilf, Electronic spectra, photochemistry, and autoxidation mechanism of the sulfite-bisulfite-pyrosulfite systems. SO_2^-, SO_3^-, SO_4^-, and SO_5^- radicals, J. Am. Chem. Soc. 94 (1972) 47–57.

[198] M. Saran, Determination of sulfite radical ($SO_3^{\bullet-}$) reaction rate constants by means of competition kinetics, Radiat. Environ. Bioph. 26 (1987) 289–294.

[199] P. Neta, R.E. Huie, One-electron redox reactions involving sulfite ions and aromatic amines, J. Phys. Chem. 89 (1985) 1783–1787.

[200] T. Luo, Y. Yuan, D. Zhou, L. Luo, J. Li, F. Wu, The catalytic role of nascent Cu $(OH)_2$ particles in the sulfite-induced oxidation of organic contaminants, Chem. Eng. J. 363 (2019) 329–336.

[201] H. Li, C. Shan, B. Pan, Fe(III)-doped g-C_3N_4 mediated peroxymonosulfate activation for selective degradation of phenolic compounds via high-valent iron-oxo species, Environ. Sci. Technol. 52 (2018) 2197–2205.

[202] S.Y. Pang, J. Jiang, J. Ma, Oxidation of sulfoxides and arsenic(III) in corrosion of nanoscale zero valent iron by oxygen: Evidence against ferryl ions (Fe(IV)) as active intermediates in Fenton reaction, Environ. Sci. Technol. 45 (2011) 307–312.

[203] Z. Wang, J. Jiang, S. Pang, Y. Zhou, C. Guan, Y. Gao, J. Li, Y. Yang, W. Qiu, C. Jiang, Is sulfate radical really generated from peroxydisulfate activated by iron (II) for environmental decontamination? Environ. Sci. Technol. 52 (2018) 11276–11284.

[204] Y. Gao, Y. Zhou, S.Y. Pang, J. Jiang, Z. Yang, Y. Shen, Z. Wang, P.X. Wang, L. H. Wang, New insights into the combination of permanganate and bisulfite as a novel Advanced Oxidation Process: Importance of high valent manganese-oxo species and sulfate radical, Environ. Sci. Technol. 53 (2019) 3689–3696.

[205] Z. Wang, W. Ma, C. Chen, H. Ji, J. Zhao, Probing paramagnetic species in titania-based heterogeneous photocatalysis by electron spin resonance (ESR) spectroscopy-A mini review, Chem. Eng. J. 170 (2011) 353–362.

[206] X. Peng, Y.L. Xiong, B. Kong, Antioxidant activity of peptide fractions from whey protein hydrolysates as measured by electron spin resonance, Food. Chem. 113 (2009) 196–201.

[207] Y. Bao, J. Huang, G. Cagnetta, G. Yu, Removal of F–53B as PFOS alternative in chrome plating wastewater by UV/Sulfite reduction, Water Res. 163 (2019), 114907.

[208] X. Duan, H. Sun, S. Wang, Metal-free carbocatalysis in advanced oxidation reactions, Acc. Chem. Res. 51 (2018) 678–687.

[209] J. Yu, H. Feng, L. Tang, Y. Pang, G. Zeng, Y. Lu, H. Dong, J. Wang, Y. Liu, C. Feng, J. Wang, B. Peng, S. Ye, Metal-free carbon materials for persulfate-based advanced oxidation process: Microstructure, property and tailoring, Prog. Mater. Sci. 111 (2020), 100654.

[210] J. Guo, X. Jia, Q. Gao, Insight into the improvement of dewatering performance of waste activated sludge and the corresponding mechanism by biochar-activated persulfate oxidation, Sci. Total. Environ. 744 (2020), 140912.

[211] J. Guo, X. Wen, J. Yang, T. Fan, Removal of benzo(a)pyrene in polluted aqueous solution and soil using persulfate activated by corn straw biochar, J. Environ. Manag. 272 (2020), 111058.

[212] P. Xie, L. Zhang, J. Wang, Y. Zou, S. Wang, S. Yue, Z. Wang, J. Ma, Transformation of tetrabromobisphenol a in the iron ions-catalyzed auto-oxidation of HSO_3^{2-}/ SO_3^{2-} process, Sep. Purif. Technol. 235 (2020), 116197.

[213] W. Shi, Q. Cheng, P. Zhang, Y. Ding, H. Dong, L. Duan, X. Li, A. Xu, Catalytic decolorization of methyl orange by the rectorite–sulfite system, Catal. Commun. 56 (2014) 32–35.

[214] H. Eibenberger, S. Steenken, P. O'Neill, D. Schulte-Frohlinde, Pulse radiolysis and electron spin resonance studies concerning the reaction of $SO_4^{\bullet-}$ with alcohols and ethers in aqueous solution, J. Phys. Chem. 82 (1978) 749–750.

[215] S. Giannakis, K.Y.A. Lin, F. Ghanbari, A review of the recent advances on the treatment of industrial wastewaters by sulfate radical-based advanced oxidation processes (SR-AOPs), Chem. Eng. J. 406 (2021), 127083.